

QUANTUM ANTIFERROMAGNETS IN TWO DIMENSIONS

Subir Sachdev
Department of Physics
Yale University
P.O. Box 2157, Yale Station
New Haven CT 06520, U.S.A.

Lectures presented at the summer course on
‘‘Low Dimensional Quantum Field Theories for Condensed Matter Physicists’’,
24 Aug. to 4 Sep. 1992, Trieste, Italy

ABSTRACT

I review recent work, performed in collaboration primarily with N. Read and Jinwu Ye, on the properties of quantum antiferromagnets in two dimensions. The emphasis is on the properties of the antiferromagnet in states which do not have any long-range magnetic order. The universal spin dynamics in the quantum critical region of number of frustrated and random antiferromagnets is studied; implications for neutron scattering experiments in the lightly-doped cuprates are noted. The nature of the quantum-disordered phase of non-random frustrated antiferromagnets is examined in some detail: the states found have (i) collinear spin correlations, spin-Peierls or valence-bond-solid order, and confined spinons, order and confined spinons or (ii) coplanar spin correlations, no spin-Peierls order and deconfined bosonic spinons.

1. INTRODUCTION

The study of quantum antiferromagnets goes back to very early work of Bethe [1], Anderson [2] and Kubo [3]. However the subject has recently seen a tremendous amount of renewed theoretical and experimental interest. We will restrict the discussion here to antiferromagnets described by the following simple Hamiltonian:

$$\mathcal{H} = \sum_{i,j} J_{ij} \hat{\mathbf{S}}_i \cdot \hat{\mathbf{S}}_j \quad (1)$$

where the $\hat{\mathbf{S}}_i$ are spin S quantum spin operators on the sites, i , of a 2-dimensional lattice. The antiferromagnetic exchange constants, $J_{ij} > 0$, are short-ranged and possibly random.

The early work [1, 2, 3] focused on the nature of the ground states of \mathcal{H} with magnetic long-range-order (LRO): these are states in which there is a spin-condensate:

$$\langle \mathbf{S}_i \rangle = \mathbf{m}_i \neq 0 \quad (2)$$

The situation changed dramatically with the suggestion by Anderson [4] in 1987 that quantum disordered ground states of two dimensional quantum antiferromagnets are relevant to the phenomenon of high temperature superconductivity in the cuprates [5]. The magnetically disordered states are those in which

$$\langle \mathbf{S}_i \rangle = 0 \quad (3)$$

We emphasize that the spin-glass ground state is not of this type; rather it is a magnetically ordered ground state in which \mathbf{m}_i is a random function of i . The following questions arise immediately in the study of any quantum disordered phase:

- Is the quantum-disordered ground state characterized completely by Eqn. (3) ? Or are there additional broken symmetries that must be present ? Naively, one may conclude that the first of these is the most natural possibility. Many investigators have addressed this issue and found however that other broken symmetries appear more often than was initially expected. Only under special conditions, which N. Read and I delineated in Refs. [6, 7, 8], does a featureless spin-fluid state appear. This work will be reviewed in Section 6.
- What is the nature of the excitations above the ground state ? Do the individual quanta of excitations carry fractional spin quantum numbers ($S=1/2$) ? Such excitations are conventionally called spinons. A second possibility is that the spinons are always confined in pairs, leading to excitations which have only integral spin.
- If the spinons are unconfined, what are their statistics ? In non-random antiferromagnets, the spinons are usually separated from the ground state by a gap, and physical conditions with a sufficiently dilute concentration of spinons can always be defined to make the question of their statistics meaningful.

Most of the questions above will be addressed in the course of these lectures. We will use a combination of semiclassical and a number of different large- N expansions to address these issues. In particular, much will be learned by comparing and reconciling the results of the different expansions.

There are several motivations for addressing these and other related questions:

- The cuprates undergo a transition to a quantum disordered ground state upon doping with a small concentration of mobile holes. In $La_{2-x}Sr_xCuO_4$ this occurs somewhere between $x = 0.02$ and $x = 0.07$. At lower dopings the holes are localized and a Hamiltonian as in (1) is adequate. At larger dopings the holes become mobile, requiring study of quantum-disordered antiferromagnets in the presence of propagating holes. A number of neutron scattering experiments have given us a detailed picture of the spin dynamics of these antiferromagnets [9, 10, 11, 12, 13, 14, 15, 16], much of which is poorly understood.
- The spin-1/2 antiferromagnet on a kagomé lattice may possess a quantum disordered phase. Recently there have been a number of experimental realizations of Heisenberg antiferromagnets on a kagomé lattice: the layered kagomé antiferromagnets $SrCr_{8-x}Ga_{4+x}O_{19}$, $KCr_3(OH)_6(SO_4)_2$ [17, 18, 19] and layers of 3He on graphite [20, 21].

As noted above, there have been a number of detailed dynamic neutron scattering experiments on lightly-doped cuprates [9, 10, 11, 12, 13, 14, 15, 16] and layered frustrated antiferromagnets [20, 21, 17, 18, 19]. One feature of the dynamic neutron scattering on the lightly-doped cuprates ($La_{2-x}Sr_xCuO_4$ for $0.02 < x < 0.05$) that is particularly intriguing is that the overall frequency scale of the spin excitation spectrum appears to be given simply by the absolute temperature. In particular, it appears to be independent of all microscopic energy scales *e.g.* an antiferromagnetic exchange constant.

We have recently proposed [22] that this anomalous dynamics is a very general property of finite T , spin fluctuations in the quantum-critical [23] region. This is the region in the temperature-coupling constant plane where the spin fluctuations are controlled by the critical fixed point between the magnetically ordered and the quantum disordered phase. The antiferromagnet notices the thermal deviation from $T = 0$ at a scale shorter than that at which it notices that the coupling constants are not exactly critical. The system is neither fully ordered or fully disordered at long distances, but remains in limbo controlled by the critical point between them; the dynamics exhibits features of both phases and the energy scale is set solely by the absolute temperature. In our work [22] universal scaling functions and exponents for the quantum-critical dynamics of frustrated, doped, and random antiferromagnets have been proposed. Complete scaling functions and exponents have been calculated for a model system - non-random, frustrated two-dimensional Heisenberg antiferromagnets with a vector order-parameter. These results will be reviewed in Sections 4 and 5 and represent the first calculation of dynamic scaling functions in a two-dimensional quantum phase transition.

Most of the work reviewed here will be on non-random two-dimensional antiferromagnets. There will however be a limited discussion of the consequences of randomness in Section 5. For the most part, random quantum antiferromagnets are only very poorly understood; there has however been some recent progress [24, 25] for which the reader is invited to consult the original papers.

We will begin this review with a derivation of the coherent-state, path-integral formulation of quantum antiferromagnets. The representation of the semiclassical fluctuations of antiferromagnets by the non-linear sigma model will be discussed in Section 3. In Section 4, the properties of the $O(M)$ non-linear sigma model will be studied in a large- M theory, with a particularly emphasis on the quantum-critical region. This will lead to a more general discussion of quantum-criticality in Section 5. Finally the quantum disordered state will be discussed in Section 6.

2. COHERENT STATE PATH INTEGRAL

In this section we shall present a derivation of a coherent state path integral formulation of the dynamics of a generic antiferromagnetic. There will be no approximations made and the results are essentially exact. As identical manipulations have to be performed on all the spins of the antiferromagnet, we will drop the site index in the following and simply present the path integral formulation for a single spin. The path integral for the lattice problem will involve direct copies of the single site result. The results of this section are “well-known”, although the formulation here was first discussed in Ref. [26]; it has the advantage of explicitly preserving spin-rotation invariance.

As a first step, we need to define the spin coherent states. The reader is urged at this point to consult the very instructive discussion on the properties and uses of coherent states in general in the introduction to the book edited by Klauder [27]. We restrict our discussion here to the case of $SU(2)$ spins. The conventional complete basis for the spin states at each site is the usual one corresponding to the eigenstates of $\hat{\mathbf{S}}^2$ and \hat{S}_z :

$$|S, m\rangle \quad \text{with } m = -S \dots S \quad (4)$$

In the path-integral formulation it is more convenient to use instead an overcomplete basis of states $|\mathbf{N}\rangle$ labeled by the points \mathbf{N} on the surface of the unit sphere. These states are normalized, $\langle \mathbf{N} | \mathbf{N} \rangle = 1$ but are not mutually orthogonal. Their crucial properties are that the expectation value of the spin is given by

$$\langle \mathbf{N} | \hat{\mathbf{S}} | \mathbf{N} \rangle = S \mathbf{N}, \quad (5)$$

and the completeness relation

$$\int \frac{d\mathbf{N}}{2\pi} |\mathbf{N}\rangle \langle \mathbf{N}| = 1, \quad (6)$$

where the integral is over the unit sphere. For $\mathbf{N} = (0, 0, 1)$, the state $|\mathbf{N}\rangle$ is easy to determine; we have

$$|\mathbf{N} = (0, 0, 1)\rangle = |S, m = S\rangle \equiv |\Psi_0\rangle \quad (7)$$

We have defined this particular coherent state as a reference state $|\Psi_0\rangle$ as it will be needed frequently in the following. For other values of \mathbf{N} we can obtain $|\mathbf{N}\rangle$ by a $SU(2)$ rotation of $|\Psi_0\rangle$. It is not difficult to show in this manner that

$$|\mathbf{N}\rangle = \exp\left(z\hat{S}_+ - z^*\hat{S}_-\right) |\Psi_0\rangle \quad (8)$$

where the relationship between the complex number z and \mathbf{N} is simplest in spherical coordinates:

$$\mathbf{N} = (\sin\theta \cos\phi, \sin\theta \sin\phi, \cos\theta) \quad (9)$$

$$z = -\frac{\theta}{2} \exp(-i\phi) \quad (10)$$

The validity of the Eqn. (7) determining the expectation value of $\hat{\mathbf{S}}$ can be verified in a straightforward manner.

It will be useful for our subsequent formulation to rewrite the above results in a somewhat different manner, making the $SU(2)$ symmetry more manifest. Define the 2×2 matrix of operators $\hat{\mathcal{S}}$ by

$$\hat{\mathcal{S}} = \begin{pmatrix} \hat{S}_z & \hat{S}_x - i\hat{S}_y \\ \hat{S}_x + i\hat{S}_y & -\hat{S}_z \end{pmatrix}. \quad (11)$$

Then Eqn. (7) can be rewritten as

$$\langle \mathbf{N} | \hat{\mathcal{S}}_{\alpha\beta} | \mathbf{N} \rangle = SQ_{\alpha\beta}, \quad (12)$$

where the matrix Q is

$$Q = \begin{pmatrix} N_z & N_x - iN_y \\ N_x + iN_y & -N_z \end{pmatrix} \equiv \mathbf{N} \cdot \vec{\sigma} \quad (13)$$

where $\vec{\sigma}$ are the Pauli matrices. Furthermore there is a simple relationship between Q and the complex number z . In particular, if we use the spin-1/2 version of the operator in Eqn. (8)

$$U = \exp \left[\begin{pmatrix} 0 & z \\ -z^* & 0 \end{pmatrix} \right] \quad (14)$$

(U is thus a 2×2 matrix), then we find

$$Q = U\sigma_z U^\dagger \quad (15)$$

We now proceed to the derivation of the coherent state path integral for the partition function

$$Z = \text{Tr} \exp(-\beta \mathcal{H}(\hat{\mathbf{S}})) \quad (16)$$

where we have emphasized that the Hamiltonian \mathcal{H} is a function of the spin operator $\hat{\mathbf{S}}$; we will restrict the following discussion to Hamiltonians in which \mathcal{H} is a linear function of any given $\hat{\mathbf{S}}$ on a fixed site. The \mathcal{H} in Eqn. (1) is certainly of this type. The transformation of Z into a path-integral begins with a standard procedure: we will omit the details of some steps, referring the reader to the introductory article in the book edited by Klauder [27]. Briefly, the exponential in Eqn. (16) is written as the Trotter product of a large number of exponentials each evolving the system over an infinitesimal imaginary-time interval $\Delta\tau$; the identity (6) is inserted between all the exponentials and the matrix elements evaluated using (5). This yields the result may now be used to obtain the following representation for the partition function

$$Z = \int \mathcal{D}\mathbf{N}(\tau) \exp \left\{ \int_0^\beta d\tau \left[\langle \mathbf{N}(\tau) | \frac{d}{d\tau} | \mathbf{N}(\tau) \rangle - \mathcal{H}(S\mathbf{N}(\tau)) \right] \right\}, \quad (17)$$

where $\mathcal{H}(S\mathbf{N})$ is obtained by replacing every occurrence of $\hat{\mathbf{S}}$ in the Hamiltonian by $S\mathbf{N}$. The first term in the action is the Berry phase term, S_B , and represents the overlap between the coherent states at two infinitesimally separated times. It can be shown straightforwardly from the normalization condition $\langle \mathbf{N} | \mathbf{N} \rangle = 1$ that S_B must be pure imaginary. In the remainder of this section we will manipulate S_B into a physically more transparent form using the expressions above for the coherent states.

Clearly, the τ -dependence of $\mathbf{N}(\tau)$ implies a τ dependent $z(\tau)$ through (10). From (8) we have therefore

$$\frac{d}{d\tau} | \mathbf{N}(\tau) \rangle = \frac{d}{d\tau} \exp \left(z(\tau) \hat{S}_+ - z^*(\tau) \hat{S}_- \right) | \Psi_0 \rangle \quad (18)$$

Taking this derivative is however not so simple: I remind you that if an operator M does not commute with its derivative $dM/d\tau$ then

$$\frac{d}{d\tau} \exp(M) \neq \frac{dM}{d\tau} \exp(M) \quad (19)$$

A careful analysis in fact leads to the general result [28]

$$\frac{d}{d\tau} \exp(M) = \int_0^1 du \exp(M(1-u)) \frac{dM}{d\tau} \exp(Mu), \quad (20)$$

where u is just a dummy integration variable. Using (18) and (20) we find

$$\begin{aligned} S_B &= \int_0^\beta d\tau \langle \mathbf{N}(\tau) | \frac{d}{d\tau} | \mathbf{N}(\tau) \rangle \\ &= \int_0^\beta d\tau \int_0^1 du \langle \mathbf{N}(\tau, u) | \left(\frac{\partial z}{\partial \tau} \hat{S}_+ - \frac{\partial z^*}{\partial \tau} \hat{S}_- \right) | \mathbf{N}(\tau, u) \rangle \end{aligned} \quad (21)$$

where $\mathbf{N}(\tau, u)$ is defined by

$$|\mathbf{N}(\tau, u)\rangle = \exp\left(u\left(z(\tau)\hat{S}_+ - z^*(\tau)\hat{S}_-\right)\right)|\Psi_0\rangle \quad (22)$$

From this definition, three important properties of $\mathbf{N}(\tau, u)$ are immediately apparent

$$\begin{aligned} \mathbf{N}(\tau, u = 1) &\equiv \mathbf{N}(\tau) \\ \mathbf{N}(\tau, u = 0) &= (0, 0, 1) \end{aligned} \quad (23)$$

$\mathbf{N}(\tau, u)$ moves with u along the great circle between $\mathbf{N}(\tau, u = 0)$ and $\mathbf{N}(\tau, u = 1)$

We can visualize the dependence on u by imagining a string connecting the physical value of $\mathbf{N}(\tau) = \mathbf{N}(\tau, u = 1)$ to the North pole, along which u decreases to 0. We can also define a u -dependent $Q(\tau, u)$ from Eqn. (13); furthermore, if we choose

$$U(\tau, u) = \exp\left[u\begin{pmatrix} 0 & z \\ -z^* & 0 \end{pmatrix}\right] \quad (24)$$

then the relationship (15) remains valid for all u . Now we use the expression (12) for the expectation value of $\hat{\mathbf{S}}$ in any coherent state to obtain

$$S_B = S \int_0^\beta d\tau \int_0^1 du \left[\frac{\partial z}{\partial \tau} Q_{21}(\tau, u) - \frac{\partial z^*}{\partial \tau} Q_{12}(\tau, u) \right], \quad (25)$$

As everything is a periodic function of τ , we may freely integrate this expression by parts and obtain

$$S_B = -S \int_0^\beta d\tau \int_0^1 du \text{Tr} \left[\begin{pmatrix} 0 & z(\tau) \\ -z^*(\tau) & 0 \end{pmatrix} \partial_\tau Q(\tau, u) \right]. \quad (26)$$

where the trace is over the 2×2 matrix indices. The definitions (15) and (24) can be used to easily establish the identity

$$\begin{pmatrix} 0 & z(\tau) \\ -z^*(\tau) & 0 \end{pmatrix} = -\frac{1}{2} Q(\tau, u) \frac{\partial Q(\tau, u)}{\partial u}, \quad (27)$$

which when inserted into (26) yields the expression for S_B in one of its final forms

$$S_B = \int_0^\beta d\tau \int_0^1 du \left[\frac{S}{2} \text{Tr} \left(Q(\tau, u) \frac{\partial Q(\tau, u)}{\partial u} \frac{\partial Q(\tau, u)}{\partial \tau} \right) \right] \quad (28)$$

An expression for S_B solely in terms of $\mathbf{N}(\tau, u)$ can be obtained by substituting in (13); this yields finally:

$$S_B = iS \int_0^\beta d\tau \int_0^1 du \mathbf{N} \cdot \left(\frac{\partial \mathbf{N}}{\partial u} \times \frac{\partial \mathbf{N}}{\partial \tau} \right) \quad (29)$$

This expression has a simple geometric interpretation: it is simply iS times the area on the surface of a unit sphere swept out by the string connecting $\mathbf{N}(\tau)$ to the North Pole - this is also the oriented area contained within the closed loop defined by $\mathbf{N}(\tau)$, $0 \leq \tau \leq \beta$, $\mathbf{N}(0) = \mathbf{N}(\tau)$ on the sphere. Note that the u dependence has dropped out of this result which only depends on the values of $\mathbf{N}(\tau, u = 1)$.

3. NON-LINEAR SIGMA MODEL

We shall now obtain a long-wavelength, large- S description of the dynamics of d -dimensional antiferromagnets in the vicinity of a ground state with collinear long-range Néel order. This description takes the form of an imaginary-time functional integral over an action which includes a non-linear sigma model field theory in $d+1$ dimensions; this result was first noted by Haldane [29, 30, 31]. The advantage of this approach is that it is the physically most transparent, and often the simplest, way of describing many of the results. Furthermore, although the derivation depends upon a semiclassical, large- S limit, all of the results have also been obtained in alternative large- N methods [26, 34, 35] which are valid well into the quantum-disordered phase. The chief disadvantages of the present approach are that it cannot simply describe the appearance of spin-Peierls order in the quantum-disordered phase, and it does not have a simple extension to a description of the phases with short-range or long-range incommensurate spin correlations.

Let us consider an antiferromagnet on a d -dimensional hypercubic lattice with only a nearest-neighbor exchange interaction J . In the semiclassical limit, the spins will predominantly orient themselves in opposite directions on the two sublattices. Let $\mathbf{n}(\mathbf{r}, \tau)$ be a continuum field of unit length which describes the local orientation of this Néel ordering - \mathbf{n} varies slowly on the scale of a lattice spacing, but the values of \mathbf{n} on well separated points can be considerably different, leaving open the possibility of a quantum disordered phase with no long-range spin order. It will turn out to be necessary to also include a component of the spins which is perpendicular to the local orientation of the Néel order - this is described by the continuum field $\mathbf{L}(\mathbf{r}, \tau)$. We have therefore on the site i of the lattice

$$\mathbf{N}(i) \approx \varepsilon_i \mathbf{n}(\mathbf{r}_i) \sqrt{1 - a^{2d} \mathbf{L}^2(\mathbf{r}_i)} + a^d \mathbf{L}(\mathbf{r}_i), \quad (30)$$

where ε_i equals ± 1 on the two sublattices, a is the lattice spacing, and

$$\mathbf{n}^2 = 1 \quad \mathbf{n} \cdot \mathbf{L} = 0 \quad \mathbf{L}^2 \ll a^{-2d} \quad (31)$$

This relationship holds for all values of τ and u , and \mathbf{n}, \mathbf{L} satisfy the same boundary conditions in u as \mathbf{N} . We insert the decomposition for \mathbf{N} into $\mathcal{H}(\mathbf{N}(\tau))$ and expand the result in gradients and powers of \mathbf{L} . This yields

$$\begin{aligned} \mathcal{H} &= \frac{1}{2} \int d^d \mathbf{r} \left[JS^2 a^{2-d} (\nabla_{\mathbf{r}} \mathbf{n})^2 + 2dJS^2 a^d \mathbf{L}^2 \right] \\ &\equiv \frac{1}{2} \int d^d \mathbf{r} \left[\rho_s (\nabla_{\mathbf{r}} \mathbf{n})^2 + \chi_{\perp} S^2 \mathbf{L}^2 \right] \end{aligned} \quad (32)$$

the second equation defines the thermodynamic spin-wave stiffness, ρ_s , and the transverse susceptibility χ_{\perp} . If we had used a different form for \mathcal{H} with modified short-range exchange

interactions, the continuum limit of \mathcal{H} would have been the same but with new values of ρ_s and χ_\perp .

To complete the expression for the coherent state path-integral in the the continuum limit we also need the expression for S_B in terms of \mathbf{n}, \mathbf{L} . We insert (30) into the (29) and retain terms upto linear order in \mathbf{L} : this yields

$$S_B = S'_B + iS \int d^d \mathbf{r} \int_0^\beta d\tau \int_0^1 du \left[\mathbf{n} \cdot \left(\frac{\partial \mathbf{n}}{\partial u} \times \frac{\partial \mathbf{L}}{\partial \tau} \right) + \mathbf{n} \cdot \left(\frac{\partial \mathbf{L}}{\partial u} \times \frac{\partial \mathbf{n}}{\partial \tau} \right) + \mathbf{L} \cdot \left(\frac{\partial \mathbf{n}}{\partial u} \times \frac{\partial \mathbf{n}}{\partial \tau} \right) \right] \quad (33)$$

where

$$S'_B = iS \sum_i \varepsilon_i \int_0^\beta d\tau \int_0^1 du \mathbf{n}_i \cdot \left(\frac{\partial \mathbf{n}_i}{\partial u} \times \frac{\partial \mathbf{n}_i}{\partial \tau} \right) \quad (34)$$

The continuum limit of S'_B is not simple due to the presence of the rapidly oscillating prefactor ε_i . In two spatial dimensions, a careful examination by several investigators [32] showed that this term is identically zero for all smooth spin configurations. However when singular spin configurations are permitted, there can be a net Berry phase [33]; this will be studied in Section 6.C. We also note in passing that in one-dimensional antiferromagnets [29] it is S'_B which gives rise to the topological θ -term.

The remainder of S_B can be simplified further. Using the fact that the vectors \mathbf{L} , $\partial \mathbf{n} / \partial \tau$, $\partial \mathbf{n} / \partial u$ are all perpendicular to \mathbf{n} and hence lie in a plane and have a vanishing triple product we find

$$S_B = S'_B + iS \int d^d \mathbf{r} \int_0^\beta d\tau \int_0^1 du \left[\frac{\partial}{\partial \tau} \left(\mathbf{n} \cdot \left(\frac{\partial \mathbf{n}}{\partial u} \times \mathbf{L} \right) \right) + \frac{\partial}{\partial u} \left(\mathbf{n} \cdot \left(\mathbf{L} \times \frac{\partial \mathbf{n}}{\partial \tau} \right) \right) \right] \quad (35)$$

The total τ derivative yields 0 as all fields are periodic in τ , while the total u derivative yields a surface contribution at $u = 1$. This gives finally

$$S_B = S'_B - iS \int d^d \mathbf{r} \int_0^\beta d\tau \mathbf{L} \cdot \left(\mathbf{n} \times \frac{\partial \mathbf{n}}{\partial \tau} \right) \quad (36)$$

Putting together (32) and (36) we obtain the following continuum limit path-integral for the antiferromagnet

$$\begin{aligned} Z &= \int \mathcal{D}\mathbf{n} \mathcal{D}\mathbf{L} \exp(S_n) \\ S_n &= S'_B - \frac{1}{2} \int_0^\beta d\tau \int d^d \mathbf{r} \left[\rho_s (\nabla_{\mathbf{r}} \mathbf{n})^2 + \chi_\perp S^2 \mathbf{L}^2 + 2iS \mathbf{L} \cdot \left(\mathbf{n} \times \frac{\partial \mathbf{n}}{\partial \tau} \right) \right] \end{aligned} \quad (37)$$

The functional integral over \mathbf{L} is simply a gaussian and can therefore be carried out

$$S_n = S'_B + \frac{1}{2} \int_0^\beta d\tau \int d^d \mathbf{r} \rho_s \left[(\nabla_{\mathbf{r}} \mathbf{n})^2 + \frac{1}{c^2} (\partial_\tau \mathbf{n})^2 \right], \quad (38)$$

where the spin-wave velocity $c = \sqrt{\rho_s \chi_\perp}$. This is the action for a $d+1$ dimensional non-linear sigma model with a residual Berry phase term. As already noted, the Berry phase terms only makes a non-zero contribution for topologically non-trivial spin configurations.

4. $O(M)$ NON-LINEAR SIGMA MODEL FOR LARGE M

We will now study the properties of the $O(M)$ non-linear sigma model field theory in a $1/M$ expansion; such an expansion was carried out for the two-dimensional model by Polyakov [36]. The results in this section represent work carried out with Jinwu Ye [22, 37].

As we have seen in the previous section, the $O(3)$ non-linear sigma model, combined with some additional Berry phase terms, describes the long-wavelength dynamics of the $SU(2)$ antiferromagnet in the semiclassical limit. The Berry phases will be completely ignored in this section - their consequences will be considered later. Furthermore, the $O(M)$ model for $M > 3$ is not simply related to any quantum antiferromagnet. Our main motivation for looking at this model is that, with proper interpretation, it presents the simplest way at arriving at some of the basic results and exploring crude features of the phase diagram of the $SU(2)$ antiferromagnet. The omitted Berry phases do induce important differences between the $SU(2)$ antiferromagnet and the $O(3)$ non-linear sigma model - these will be explored in subsequent subsections.

In this section, we will deal exclusively with the following non-linear sigma model field theory

$$Z = \int \mathcal{D}n_a \delta(n_a^2 - 1) \exp \left(-\frac{M}{2g} \int d^2\mathbf{r} \int_0^{c\beta} d\tilde{\tau} [(\nabla_{\mathbf{r}} n_a)^2 + (\partial_{\tilde{\tau}} n_a)^2] \right), \quad (39)$$

where the index a runs from 1 to M . This action can be obtained from the semiclassical action for the antiferromagnet (38) by omitting the Berry phase term S'_B , and introducing the rescaled time $\tilde{\tau} = c\tau$. We will henceforth omit the tilde on the τ and use units in which $c = 1$ - it is trivial to reinsert appropriate factors of c in the final results. The coupling constant g is given by

$$\begin{aligned} g &= \frac{Mc}{\rho_s} \\ &= \frac{6a}{S} \text{ for the large } S \text{ } SU(2) \text{ antiferromagnet in } d = 2 \end{aligned} \quad (40)$$

The large M analysis of Z begins with the introduction of the rescaled field

$$\tilde{n}_a = \sqrt{M} n_a \quad (41)$$

and the imposition of the constraint by a Lagrange multiplier λ . This transforms Z into

$$Z = \int \mathcal{D}\tilde{n}_a \mathcal{D}\lambda \exp \left(-\frac{1}{2g} \int d^2\mathbf{r} \int_0^\beta d\tau [(\nabla_{\mathbf{r}} \tilde{n}_a)^2 + (\partial_\tau \tilde{n}_a)^2 + i\lambda(\tilde{n}_a^2 - M)] \right), \quad (42)$$

This action is quadratic in the n_a , which can therefore be integrated out. This induces an effective action for the λ field which has the useful feature of having all its M dependence in a

prefactor. Therefore, for large M the λ functional integral can be evaluated by an expansion about its saddle point.

Let us look more carefully at the solution at $M = \infty$ when the saddle point action is the exact answer. At the saddle point we parametrize

$$i\langle\lambda\rangle = m^2 \quad (43)$$

where m is a function of g, T , and an upper cutoff which will be determined below. The correlator of the n_a field is the staggered dynamic spin susceptibility and is given by

$$\chi(\mathbf{k}, \omega_n) = \langle n_a(\mathbf{k}, \omega_n) n_a(-\mathbf{k}, -\omega_n) \rangle = \frac{g}{\mathbf{k}^2 + \omega_n^2 + m^2} \quad (44)$$

where we have introduced the momentum \mathbf{k} and the Matsubara frequency ω_n . Neutron scattering experiments yield a direct measurement of the imaginary part of χ (χ'') for real frequencies. At $M = \infty$, analytic continuation of the above result yields

$$\chi''(\mathbf{k}, \omega) = \frac{g\pi}{2\sqrt{\mathbf{k}^2 + m^2}} \left(\delta(\omega - \sqrt{\mathbf{k}^2 + m^2}) - \delta(\omega + \sqrt{\mathbf{k}^2 + m^2}) \right) \quad (45)$$

Another quantity often accessed in neutron scattering is the momentum integrated local susceptibility, χ_L , which is given by

$$\chi_L''(\omega) = \int \frac{d^2\mathbf{k}}{4\pi^2} \chi''(\mathbf{k}, \omega) = \frac{g}{4} (\theta(\omega - m) - \theta(-\omega - m)) \quad (46)$$

where $\theta(x)$ is the stop function which is non-zero only for positive x . An important shortcoming of the $M = \infty$ result is the absence of any damping which is always present at finite T - this only appears at order $1/M$ which will be discussed later. The damping will broaden the delta function peaks in $\chi(\mathbf{k}, \omega)$ and fill in the gap region ($|\omega| < m$) in $\chi_L(\omega)$ at all finite temperatures and all values of g - true delta functions and gaps can however survive at $T = 0$. We can also examine the spin structure factor, $S(\mathbf{k})$ which is the equal-time spin-spin correlation function in momentum space

$$\begin{aligned} S(\mathbf{k}) &= T \sum_{\omega_n} \langle n_a(\mathbf{k}, \omega_n) n_a(-\mathbf{k}, -\omega_n) \rangle \\ &= \frac{g}{2\sqrt{\mathbf{k}^2 + m^2}} \coth \left(\frac{\sqrt{\mathbf{k}^2 + m^2}}{2T} \right) \end{aligned} \quad (47)$$

The spin-correlation length, ξ , is therefore given by

$$\begin{aligned} \xi^2 &\equiv -\frac{1}{S(0)} \left. \frac{\partial S}{\partial \mathbf{k}^2} \right|_{\mathbf{k}=0} \\ &= \frac{1}{m^2} \left(\frac{1}{2} + \frac{m/T}{2 \sinh(m/T)} \right) \end{aligned} \quad (48)$$

The factor multiplying $1/m^2$ decreases monotonically from 1 to $1/2$ as m/T increases from 0. Thus m is essentially the inverse spin correlation length, apart from an innocuous numerical factor between 1 and $1/\sqrt{2}$.

We now determine m . The saddle-point equation is simply the constraint $n_a^2 = 1$, or more explicitly

$$T \sum_{\omega_n} \int \frac{d^2\mathbf{k}}{4\pi^2} \frac{g}{\mathbf{k}^2 + \omega_n^2 + m^2} = 1 \quad (49)$$

where $T = 1/\beta$ is the temperature (we are using units in which $k_B = \hbar = 1$). It is easy to see that this equation is divergent in the ultraviolet, and it is therefore necessary to introduce an ultraviolet cut-off in the momentum integration. The most convenient method is to use a Pauli-Villars cut-off Λ . This transforms the constraint equation into

$$T \sum_{\omega_n} \int_0^\infty \frac{d^2\mathbf{k}}{4\pi^2} \left(\frac{g}{\mathbf{k}^2 + \omega_n^2 + m^2} - \frac{g}{\mathbf{k}^2 + \omega_n^2 + \Lambda^2} \right) = 1 \quad (50)$$

The momentum integration can be carried out and yields

$$\frac{gT}{4\pi} \sum_{\omega_n} \ln \left(\frac{\omega_n^2 + \Lambda^2}{\omega_n^2 + m^2} \right) = 1 \quad (51)$$

The frequency summation can be done exactly to give

$$\frac{gT}{2\pi} \ln \left(\frac{\sinh(\Lambda/2T)}{\sinh(m/2T)} \right) = 1 \quad (52)$$

Finally, we can solve for the dependence of m on T, g , and Λ

$$m = 2T \operatorname{Arcsinh} \left(\exp \left(-\frac{2\pi}{gT} \right) \sinh \left(\frac{\Lambda}{2T} \right) \right) \quad (53)$$

A remarkable amount of information is contained in this innocuous looking equation. By examining the $T \rightarrow 0$ limit of this equation, it is immediately apparent that the behavior of m is quite different depending upon whether g is smaller, larger, or close to a critical value g_c given by

$$g_c = \frac{4\pi}{\Lambda} \quad (54)$$

We examine the three different phases separately.

Ordered Phase - $g < g_c$

For $g < g_c$ we find for small T that

$$m \sim \xi^{-1} \sim 2T \exp \left(-\frac{2\pi}{T} \left(\frac{1}{g} - \frac{1}{g_c} \right) \right) \quad (55)$$

Thus the correlation length diverges exponentially as $T \rightarrow 0$ and long-range-Néel order appears at $T = 0$. A renormalization group analysis of the non-linear sigma model by Chakraborty *et. al.* [23] yielded the same functional dependence of the correlation length on T ; this agreement gives us some confidence on the utility of the present large M expansion. We refer the reader to Ref. [23] for further discussion on the dynamic properties of the ordered phase - the semiclassical approach discussed there is a little more convenient for analyzing this region.

Quantum Disordered Phase - $g > g_c$

We now find for small T that

$$m \sim \frac{1}{2\xi} \sim \frac{4\pi(g - g_c)}{gg_c} \quad (56)$$

with exponentially small corrections at low T . In this case there is a finite correlation length at $T = 0$. Furthermore the excitation spectrum has an energy gap $= cm$. The low-lying excitations are the massive spin-1 (for $O(3)$) n_a quanta -they are thus triply degenerate. There will also be a spinless collective mode with a gap represented by the fluctuations of λ about its saddle-point value.

As g approaches g_c we expect on general scaling grounds that

$$\xi \sim |g - g_c|^{-\nu} \quad (57)$$

Comparing with (56) we have $\nu = 1$ at $M = \infty$. We have considered the $1/M$ corrections to this result. The structure of the perturbation theory is very similar to the $1/M$ expansion for soft-spin Ginzburg Landau models as discussed in the book by Ma [38]; we will therefore omit the details. We find

$$\nu = 1 - \frac{32}{3\pi^2 M} \quad (58)$$

Critical Region - $g \approx g_c$

In this region both $\delta g = g - g_c$ and T are small, and their ratio can be arbitrary. Before examining the result (53) let us see what can be predicted on general scaling grounds for general M . At $g = g_c$ and $T = 0$ we have a quantum field theory at its critical point. Turning on a finite T is equivalent to placing this critical system in a box which is finite in the imaginary time direction, while tuning g away from g_c at $T = 0$ induces a finite correlation length which scales like (57). The behavior of ξ for both T finite and $g \neq g_c$ is therefore predicted by the principles of finite-size scaling (after restoring factors of \hbar, c , and

Figure 1: The universal function $X(x)$ for the critical behavior of the spin-correlation length at $M = \infty$. $X(0)$ is close to, but not exactly, unity

k_b)

$$\xi = \frac{\hbar c}{k_B T} X \left(a_1 \frac{\text{sgn}(g - g_c) |g - g_c|^\nu}{T} \right) \quad (59)$$

where a_1 is the only non-universal, cutoff dependent quantity and $X(x)$ is a universal function. $X(x)$ is a smooth function of x except at $x = 0$ where it is continuous but not differentiable. It is not difficult to see that the $M = \infty$ Eqns. (48) and (53) can be written in this form with $\nu = 1$, $a_1 = 2\pi/g_c^2$ and $X(x)$ is defined by the following equations

$$\begin{aligned} X(x) &= \frac{1}{f(x)} \left(\frac{1}{2} + \frac{f(x)}{2 \sinh(f(x))} \right)^{1/2} \\ f(x) &= 2 \ln \left(\frac{e^x + \sqrt{4 + e^{2x}}}{2} \right) \end{aligned} \quad (60)$$

A plot of the function $X(x)$ is shown in Fig. 1.

The quantum-critical region is defined by the inequality $|\delta g|^\nu/T < 1$ (Fig 2). In this region the antiferromagnet notices that it is finite in the time direction at a scale which is shorter than which it notices that the coupling g is not exactly g_c . Thus the critical spin fluctuations are quenched at an energy scale which is determined completely by the

Figure 2: Phase diagram of \mathcal{H} in two dimensions. The magnetic LRO can be either spin-glass or Néel, and is present only at $T = 0$. The boundaries of the quantum-critical region are $T \sim |g - g_c|^{z\nu}$. For non-random \mathcal{H} which have commensurate, collinear, Néel LRO for $g < g_c$, all of the quantum-disordered region ($g > g_c$) has spin-Peierls order at $T = 0$ -this order extends to part of the quantum disordered region at finite T .

temperature and not any underlying antiferromagnetic exchange constant. In this regime we may simply put $x = 0$ in the formulae in the previous paragraph.

The full dynamic susceptibility also satisfies scaling functions in the critical region. For simplicity we will only consider them in the quantum critical region with $\delta g = 0$: the extension to finite δg is straightforward, at least at $M = \infty$. Application of finite size-scaling to the dynamic susceptibility yields

$$\chi(\mathbf{k}, \omega) = \frac{a_2}{T^{(2-\eta)}} \Phi\left(\frac{\hbar c \mathbf{k}}{k_B T}, \frac{\hbar \omega}{k_B T}\right) \quad (61)$$

where $\Phi(x, y)$ is a universal scaling function of both arguments, a_2 is the only non-universal quantity, and η is the usual critical exponent determining the decay of spin correlations at criticality. A normalization condition is necessary to fix the scale of Φ : the most convenient is to use

$$\left. \frac{\partial \Phi^{-1}}{\partial x^2} \right|_{x=0, y=0} = 1 \quad (62)$$

The scaling form for the local susceptibility χ_L is a little more subtle. If we perform the momentum integration of (61) we notice immediately that the integral is ultraviolet divergent because for large \mathbf{k} , $\chi \sim \mathbf{k}^{-2+\eta}$ and $\eta > 0$ (see below) for the present model. However this divergence is present only in the real part of χ . The imaginary part of χ will only involve excitations only on-shell and will therefore have rapidly vanishing spectral weight as $|\mathbf{k}|$

becomes much larger than ω/c , leading to a convergent momentum space integral. Therefore we have the scaling form

$$\chi_L''(\omega) = \int \frac{d^2\mathbf{k}}{4\pi^2} \chi''(\mathbf{k}, \omega) = a_3 |\omega|^\eta F\left(\frac{\hbar\omega}{k_B T}\right) \quad (63)$$

where F is a universal scaling function and a_3 is a non-universal constant. A remarkable feature of this result is that the energy scale for all the excitations in the system is set solely by the absolute temperature and is independent of any microscopic energy scale.

The results for the quantum-critical scaling functions at $M = \infty$ can be easily determined from the results of this section. We find $\eta = 0$,

$$\Phi(x, y) = \frac{1}{x^2 + \Theta^2 - (y + i\epsilon)^2} \quad (64)$$

where ϵ is a positive infinitesimal, and

$$F(y) = \frac{1}{4} (\theta(y - \Theta) - \theta(-y - \Theta)). \quad (65)$$

The quantity Θ is a pure number given by

$$\Theta = f(0) = 2 \ln\left(\frac{1 + \sqrt{5}}{2}\right) \quad (66)$$

We have computed these scaling functions to order $1/M$ [22]. This is a fairly non-trivial calculation and details will not be presented here. We present the results below which required about 40 hours of computation on a vectorized computer. Our results for $\text{Im}\Phi$ and F for $M = 3$ are summarized in Figs. 3 and 4. Note that $\text{Im}\Phi$ had a well defined (at least for large $|\mathbf{k}|$) spin-wave peak at a frequency close to $\omega = c|\mathbf{k}|$. The peak is broadened due to a universal damping arising from spin-wave interactions. Analytic forms for Φ can be obtained in various regimes. We have

$$\text{Re}\Phi^{-1} = C_Q^{-2} + x^2 + \dots \quad x, y \text{ small} \quad (67)$$

The universal number C_Q , to order $1/M$, is:

$$C_Q^{-1} = \Theta \left(1 + \frac{0.13}{N}\right) \quad (68)$$

$\text{Im}\Phi$ has a singular behavior for x, y small:

$$\text{Im}\Phi(x = 0, y) \sim \frac{1}{M} \exp\left(-\frac{3\Theta^2}{2|y|}\right) \quad (69)$$

while

$$\text{Im}\Phi(y < x) \sim \frac{1}{M} y \exp\left(-\frac{3\Theta^2}{2|x|}\right) \quad (70)$$

Figure 3: *The imaginary part of the universal susceptibility in the quantum-critical region, Φ , as a function of $x = \hbar c q / (k_B T)$ and $y = \hbar \omega / (k_B T)$ for a non-random square lattice AFM which undergoes a $T = 0$ transition from Néel LRO to a quantum-disordered phase. The results have been computed in a $1/M$ expansion to order $1/M$ and evaluated for $M = 3$. The two-loop diagrams were analytically continued to real frequencies and the integrals then evaluated numerically. The shoulder on the peaks is due to a threshold towards three spin-wave decay.*

Figure 4: *The imaginary part of the universal local susceptibility, F , for the same model as in the previous figure. We have $F(y) = y^{-\mu} \int d\vec{x} \text{Im}\Phi(\vec{x}, y)$. The oscillations at large y are due to a finite step-size in the momentum integrations.*

These peculiar singularities are probably artifacts of the large M expansion and occur only in the region $x, y < 1/M$ - the naive expectation that $\text{Im}\Phi \sim y$ for small y is probably correct. With either x, y large, Φ has the form

$$\Phi = \frac{D_Q}{(x^2 - y^2)^{1-\eta/2}} + \dots \quad ; \quad D_Q = 1 - \frac{0.3426}{N}. \quad (71)$$

The exponent η has the known [39] expansion

$$\eta = \frac{8}{3\pi^2 M} - \frac{512}{27\pi^4 M^2} > 0 \quad (72)$$

The scaling function for the local susceptibility, $F(y)$, has the limiting forms

$$F(y) = \text{sgn}(y) \frac{0.06}{N} |y|^{1-\eta} \quad y \ll 1 \quad ; \quad F(y) = \text{sgn}(y) \frac{D_Q}{4} \frac{\sin(\pi\eta/2)}{\pi\eta/2} \quad y \gg 1 \quad (73)$$

As η is small, F is almost linear at small y . Note that the finite temperature $1/M$ fluctuations have filled in the gap in the spectral functions at all frequencies. These scaling functions represent the universal dissipative dynamics of critical spin wave fluctuations.

5. QUANTUM CRITICAL DYNAMICS OF 2D ANTIFERROMAGNETS

The universal dynamic scaling forms discussed in the last section in the context of unfrustrated antiferromagnets can in fact be generalized to describe the quantum critical region of a large number of frustrated and random quantum antiferromagnets. Of course, explicit calculations of the exponents and scaling functions is much more difficult and only a few results are currently available. There has however been some very recent progress [24, 25] which will not be reviewed here.

Our motivation for considering quantum critical fluctuations in random, frustrated antiferromagnets is provided by recent neutron scattering experiments on lightly-doped $La_{2-x}Sr_xCuO_4$ where $0.02 < x < 0.07$. In this doping range it has been noted by the experimentalists [9, 11] that the dynamic spin susceptibility measured as a function of frequency, ω , and temperature T follows the following scaling form with reasonable accuracy

$$\int \frac{d^2\mathbf{k}}{4\pi^2} \chi''(\mathbf{k}, \omega) = I(|\omega|) F\left(\frac{\hbar\omega}{k_b T}\right) \quad (74)$$

Experimental results for the functions F, I from Ref. [15] are shown in Figs 5 and 6. We will argue below that the theory predicts that the prefactor I must be of the form

$$I \sim |\omega|^\mu \quad (75)$$

Figure 5: *Neutron scattering results for the scaling function F from Ref. [15]*

Figure 6: *Neutron scattering results for the normalization factor I from Ref. [15]*

where the exponent μ is expected to satisfy $-1 < \mu < 0$. A fit of this form by B. Keimer [40] to the experimental result yielded $\mu = -0.41 \pm 0.05$.

A remarkable feature of the above result for χ is that the frequency scale for the spin fluctuations is set completely by the absolute temperature. The underlying exchange constants appear to modify only the prefactor of the scaling form. We have recently proposed [22] that this scaling of the frequency scale with temperature is a rather general property of spin fluctuations of two-dimensional antiferromagnets in their quantum critical region. Let us discuss this in the context of the general Hamiltonian \mathcal{H} which we will use to model the lightly-doped cuprates. In the lightly doped region the holes are localized at low temperatures, indicating that a suitable form of \mathcal{H} will be sufficient to describe the spins. A specific form has in fact been proposed by Gooding and Mailhot [41] and yielded reasonable results on the doping dependence of the zero temperature spin correlation length.

We will find it necessary to distinguish between two different types of magnetic LRO:

(A) Néel LRO, in which case

$$\mathbf{m}_i \sim e^{i\mathbf{Q}\cdot\mathbf{R}_i} \quad (76)$$

with \mathbf{Q} the Néel ordering wavevector, and

(B) spin-glass LRO, in which case \mathbf{m}_i can have an arbitrary dependence on i , specific to the particular realization of the randomness. The lower critical dimension of the Heisenberg spin-glass [42] may be larger than 3 - in this case the spin-glass LRO will not survive to any finite T , even in the presence of a coupling between the layers. This, however, does not preclude the existence of spin-glass LRO at $T = 0$.

Consider now a $T = 0$ phase transition between the magnetic LRO and the quantum-disorder, induced by varying a coupling constant g which is dependent on the ratio's of the J_{ij} in \mathcal{H} . Let the transition occur at a critical value $g = g_c$. If the transition is second-order then there will be a diverging scale

$$\xi_g \sim |g - g_c|^{-\nu} \quad (77)$$

which is the distance at which the antiferromagnet first notices that its properties are not critical; at distances shorter than ξ_g the spin fluctuations are indistinguishable from those at criticality. For Néel LRO, ξ_g is identical at $T = 0$ to the spin correlation length ξ considered in Section 4. Therefore $1/\xi$ is the width of the peak in the spin structure-factor at the ordering wavevector \mathbf{Q} . The meaning of ξ_g is more subtle for the case of spin-glass LRO. As the condensate \mathbf{m}_i is a random function of i , there will be no narrowing of the peak in the structure-factor. However it is possible to define a diverging length scale associated with correlations the Edwards-Anderson order-parameter q_{EA} ; ξ_g will therefore be related to the decay of certain four-spin correlation functions [42].

At finite temperature and near $g = g_c$ we can define a second length scale ξ_T associated with the distances at which thermal effects become apparent. The dependence of ξ_T on T can be deduced from finite-size scaling. At $g = g_c$ the antiferromagnet is a $d + 1$ dimensional critical system which is described by a scale-invariant field theory. However, it is not necessary in general for the theory to be Lorentz invariant, as distances along the imaginary time direction can scale with a non-trivial exponent, z , with respect to spatial distances. The exponent z is also referred to as the dynamic critical exponent. As $1/T$ acts as a finite-size in the time direction we therefore expect

$$\xi_T \sim \frac{1}{T^{(1/z)}} \quad (78)$$

Now imagine that the system is in a region where $\xi_T < \xi_g$ (we assume implicitly that both these scales are much larger than the lattice spacing) which defines the quantum-critical region - see Fig. 2. The boundaries of this region are therefore specified by

$$T \sim |g - g_c|^{z\nu} \quad (79)$$

Under these circumstances the antiferromagnet will notice the finite temperature *before* it notices the deviation from the purely critical behavior at $g = g_c$. The spin-fluctuations will therefore be controlled by the repulsive flow away from the critical fixed point, cutoff by a finite scale which is set by the temperature. Both these properties are universal features of the critical fixed point and the dynamic spin susceptibility is therefore expected to obey a universal scaling form. We will study the scaling form separately for the transition from the two different types of magnetic long-range-order distinguished above:

5.A Néel order

This section generalizes the results of Section 4 to include the effects of disorder. We emphasize however that the disorder is not strong enough to destroy the small- g Néel ordered phase.

The first question which must be addressed is whether an infinitesimal amount of disorder is relevant at the fixed point describing the transition in the pure system. We begin by assuming that disorder is irrelevant. In this case the critical exponents will be unmodified. In particular the exponent ν will preserve the value $\nu = 0.705 \pm 0.005$ [43] of the pure system. However by a result of Chayes *et.al.* [44] the value of ν in any random system must satisfy

$$\nu \geq \frac{2}{d} \quad (80)$$

where d is the dimensionality of the space over which disorder is uncorrelated. In our case, disorder is uncorrelated only along the two spatial directions, which leads to $\nu \geq 1$. As

this inequality is violated by the above value of ν , our hypothesis is inconsistent. Therefore disorder is a relevant perturbation and must modify the universality class of the transition.

The random fixed-point is quite difficult to access in general, but a few of its properties can be delineated by general considerations. Firstly, the space-time anisotropy induced by disorder implies that the critical-theory need not be Lorentz invariant (unlike Section 4) and therefore

$$z \neq 1 \quad (81)$$

The results in Section 4 for the dynamic scaling form for $\chi(\mathbf{k}, \omega)$ can now be easily generalized. At $T = 0$ the static spin susceptibility, χ , will have a divergence at $g = g_c$ and wavevector $\mathbf{k} = \mathbf{Q}$:

$$\chi(\mathbf{k} = \mathbf{Q}, \omega = 0) \sim \frac{1}{|g - g_c|^\gamma} \quad (82)$$

with $\gamma = (2 - \eta)\nu$. At finite \mathbf{k}, ω, T finite-size scaling yields the scaling form [22]

$$\chi(\mathbf{k}, \omega) = \frac{a_1}{T^{(2-\eta)/z}} \Phi \left(\frac{a_2 |\mathbf{k} - \mathbf{Q}|}{T^{1/z}}, \frac{\hbar\omega}{k_B T} \right) \quad (83)$$

where a_1, a_2 are non-universal constants, and Φ is a universal, complex function of both arguments. The deviations from quantum-criticality lead to an additional dependence of Φ on ξ_T/ξ : this number is small in the QC region and has been set to 0. The scaling form for the local susceptibility can be obtained by integrating (83) over \mathbf{k} . The integral over \mathbf{k} will be convergent in the ultraviolet provided $\eta < 0$ - available results, which are discussed below, strongly indicate that all random systems in fact have $\eta < 0$. We may therefore freely integrate over \mathbf{k} and obtain

$$\chi_L''(\omega) = a_3 |\omega|^\mu F \left(\frac{\hbar\omega}{k_B T} \right) \quad (84)$$

with

$$\mu = \eta/z, \quad (85)$$

$$F(y) = y^{-\mu} \int \frac{d^2 \mathbf{x}}{4\pi^2} \text{Im} \Phi(\vec{x}, y) \quad (86)$$

a universal function, and a_3 a non-universal number. The real part χ_L' will also obey an identical scaling form as long as $\eta < 0$. The asymptotic forms for F for small and large arguments can be deduced from general considerations. For large y , or $\hbar\omega \gg k_B T$, we expect χ to become independent of T ; therefore

$$F(y) \sim \text{sgn}(y) \quad \text{for } |y| \gg 1 \quad (87)$$

For small ω , but T finite, we expect that $\chi_L'' \sim \omega$ - no anomalous scaling with ω is expected at finite temperature. Therefore

$$F(y) \sim |y|^{1-\mu} \text{sgn}(y) \quad \text{for } |y| \ll 1 \quad (88)$$

We emphasize again that all non-universal energy scales only appear in the prefactor a_3 and the frequency scale in F is determined solely by T .

Let us now examine two simple realizations of randomness in \mathcal{H} for which exponents can be estimated from the literature.

(a) *Weak bond randomness*

Take the simplest pure model which has a transition from Néel LRO to quantum disorder - we will argue in Section 6 that this is the square lattice spin-1/2 antiferromagnet with first (J_1) and second (J_2) neighbor interactions - the $J_1 - J_2$ model. The transition is expected to be described by the non-linear sigma model of Section 4. (As noted in Section 6.C, the quantum-disordered phase of this model possesses spin-Peierls LRO - it has been argued however that the coupling to the spin-Peierls order is dangerously irrelevant [22, 45, 46] and does not modify two-spin correlation functions in the quantum-critical region; the spin-Peierls order will therefore be neglected here.) Now add a small fluctuation in the J_1 bonds of the $J_1 - J_2$ model : *i.e.* $J_1 \rightarrow J_1 + \delta J_1$ where δJ_1 is random, with zero mean, and r.m.s. variance $\ll J_1$. This last condition ensures that a Néel LRO to quantum disorder transition will continue to occur as a function of J_2/J_1 . Moreover, as the disorder is weak, the mapping to the non-linear sigma model of Section 3 will continue to work, leading now to a modified partition function (39) with the coupling g a random function of \mathbf{r} . A soft-spin version of this action has been examined by Dorogovstev and Boyanovsky and Cardy [47]. They considered a field theory with a M component order parameter which had random couplings in $d = 4 - \epsilon - \epsilon_\tau$ space dimensions and ϵ_τ time dimensions. The theory was then examined in a double expansion in ϵ, ϵ_τ [47]. The expansion is poorly-behaved, and for the case of interest here ($M = 3, \epsilon = 1, \epsilon_\tau = 1$) the random fixed-point has the exponent estimates

$$\eta = -0.17, \quad z = 1.21, \quad \nu = 0.64, \quad \mu = -0.15. \quad (89)$$

Note (i) μ, η are negative, unlike the pure fixed point and (ii) ν is smaller than $2/d$, violating the required bound [44]. This latter discrepancy is not a cause for great concern as it is clear from the low-order results that the series is badly behaved and that there are large higher-order corrections.

(b) *Static holes on square lattice vertices*

Consider next a \mathcal{H} on the square lattice with only J_1 couplings, but with a small concentration of static, spinless holes on the vertices; this model will display a Néel LRO to quantum-disorder transition at a critical concentration of holes. In the coherent-state path-integral formulation of the pure model, discussed in Section 3, each spin contributes a Berry phase which is almost completely canceled in the continuum limit between the contributions of the two sublattices. The model with holes will have large regions with unequal numbers of

spins on the two sublattices: such regions will contribute a Berry phase which will almost certainly be relevant at long distances. Therefore the field theory of Ref. [47] is not expected to describe the Néel LRO to quantum-disorder transition in this case. It appears instead to be a model which possesses relevant spin configurations which have complex weights in Euclidean time, and not amenable to a field-theoretic analysis by existing methods. The only available results are those of Wan *et. al.* [48] who performed a cluster expansion in the concentration of spins *i.e.* they expanded about configurations with the maximum number of holes. Their series analysis yielded the exponents

$$\eta = -0.6, \quad z = 1.7, \quad \nu = 0.8, \quad \mu = -0.35. \quad (90)$$

Note again that $\mu, \eta < 0$, although the violation of $\nu > 2/d$ suggests problems with the series extrapolations.

5.B Spin-glass order

We now turn to the case where the degree of frustration is large enough to destroy the Néel LRO state and induce first a state with spin-glass LRO. The transition to quantum-disorder occurs subsequently from the spin-glass phase. We will argue below that the lightly doped cuprates are better described by this scenario.

Consider then the scaling of χ in the quantum-critical region of the spin-glass LRO to quantum-disorder transition. As the condensate \mathbf{m}_i is a random function of i , we do not expect any singular behavior as a function of \mathbf{k} . In particular, the scaling form (83) will not be obeyed. However, the local susceptibility $\chi_L(\omega_n)$ will be quite sensitive to the transition. In particular, χ_L measures on-site spin-correlation functions

$$\begin{aligned} \chi_L(\omega_n) &\equiv \int_0^{1/(k_B T)} d\tau e^{i\omega_n \tau} C(\tau), \\ C(\tau) &= \overline{\langle \mathbf{S}_i(0) \cdot \mathbf{S}_i(\tau) \rangle} \end{aligned} \quad (91)$$

(where the bar represents an average over all the sites i) which acquire long-range order in time in the spin-glass phase. Thus in the $T = 0$ spin-glass phase [42]

$$\lim_{\tau \rightarrow \infty} C(\tau) = \overline{\mathbf{m}_i^2} = q_{EA} > 0 \quad (92)$$

where q_{EA} is the Edwards-Anderson order-parameter. At the phase transition this order-parameter will vanish as

$$q_{EA} \sim (g_c - g)^\beta \quad (93)$$

At $T = 0$, the dynamic-scaling hypothesis then implies that near $g = g_c$

$$C(\tau) = (g_c - g)^\beta h(\tau |g - g_c|^{z\nu}) \quad (94)$$

where h is a universal scaling function which tends to a constant for large argument. For $\tau \ll |g - g_c|^{-z\nu}$, $C(\tau)$ should be independent of $g - g_c$; a standard argument then implies that at criticality

$$C(\tau) \sim \frac{1}{\tau^{\beta/(z\nu)}} \quad (95)$$

Using (91) it follows then that χ_L'' obeys a scaling form identical to (84) with the exponent μ now given by

$$\mu = -1 + \frac{\beta}{z\nu} \quad (96)$$

The function F continues to satisfy the asymptotic forms in (87) and (88). We emphasize that the above scaling forms are valid, despite the failure of the \mathbf{k} dependent scaling (83). As everything is expected to be non-singular as a function of \mathbf{k} , we in fact expect (84) to hold independently at all \mathbf{k} .

Until recently [24, 25], there were essentially no theoretical results for μ for a transition in this class. The identity (96) clearly shows $\mu > -1$. It is also plausible that $\mu < 0$. This follows from numerical studies of the quantum-disordered phase of random, spin-1/2 antiferromagnets [49] which found a divergent zero-temperature local susceptibility in the quantum-disordered phase. The susceptibility at the critical point is therefore also expected to be divergent, implying $\mu < 0$.

Finally, we return to a discussion of the experimental situation. An important property of the experiments is that the spin correlation length becomes independent of temperature, over a significant range of low temperatures. This is clearly incompatible with the presence of a $T = 0$ transition from Néel LRO to quantum-disorder which would have $\xi \sim 1/T$ at $g = g_c$. This leaves the remaining possibility of a spin-glass LRO to quantum-disorder transition.

Further support for this scenario is provided by the work of Gooding and Mailhot [41]: they considered a model of the doped cuprates in which the dopant holes are localized on the oxygen sites and the $Cu-O-Cu$ complex on that bond has been replaced by a single spin-1/2 doublet. This model leads naturally to strong frustration in the ground state. A simulation of the classical version led a $T = 0$ correlation length which was in good agreement with the experimental results. Further, their results seem to indicate that in the 2D system, Néel LRO is destroyed and spin-glass LRO appears at any non-zero concentration of dopants.

The main experimental measurements which then need to be understood are the value of $\mu = -0.41 \pm 0.05$ and the functional form of F . The fact that $\mu < 0$ verifies experimentally the theoretical prediction that disorder will destroy the pure fixed point which had $\mu > 0$. More detailed theoretical studies of quantum spin glass are clearly called for [24, 25].

6. QUANTUM DISORDERED PHASES OF NON-RANDOM 2D ANTIFERROMAGNETS

We now turn to an examination of the structure of the possible quantum-disordered phases of \mathcal{H} in the absence of randomness. Our study of these phases has so far been limited to the large M , $O(M)$ non-linear sigma model in Section 4. The structure of the quantum-disordered phase found there was rather simple: the ground state was a featureless spin-fluid with massive integer spin excitations. No half-integer spin excitations were found. We shall find upon careful examination here that this simple picture is almost never valid [6, 7]. The only exception will be even-integer antiferromagnets on the square lattice which have a two-sublattice Néel ground state in the classical limit [50]. We note however that the results on the quantum-critical dynamic scaling functions found above are not modified by any of the effects to be discussed in this section: the properties of the quantum-disordered phase are controlled by a strong-coupling fixed point while quantum criticality is determined by the critical fixed point [22].

A careful examination of the quantum-disordered phase requires an approach which is designed explicitly to be valid in a region well separated from Néel LRO; the non-linear sigma model is essentially a semiclassical expansion and can only approach the disordered phase from the the Néel state. To this end, we introduce the Schwinger boson description [51]. For the group $SU(2)$ the complete set of $(2S + 1)$ states (4) on site i are represented as follows

$$|S, m\rangle \equiv \frac{1}{\sqrt{(S+m)!(S-m)!}} (b_{i\uparrow}^\dagger)^{S+m} (b_{i\downarrow}^\dagger)^{S-m} |0\rangle. \quad (97)$$

We have introduced two flavors of bosons on each site, created by the canonical operator $b_{i\alpha}^\dagger$, with $\alpha = \uparrow, \downarrow$, and $|0\rangle$ is the vacuum with no bosons. The total number of bosons, n_b is the same for all the states; therefore

$$b_{i\alpha}^\dagger b_i^\alpha = n_b \quad (98)$$

with $n_b = 2S$ (we will henceforth assume an implied summation over repeated upper and lower indices). It is not difficult to see that the above representation of the states is completely equivalent to the following operator identity between the spin and boson operators

$$\hat{S}_{ia} = \frac{1}{2} b_{i\alpha}^\dagger \sigma_\beta^{a\alpha} b_i^\beta \quad (99)$$

where $a = x, y, z$ and the σ^a are the usual 2×2 Pauli matrices. The spin-states on two sites i, j can combine to form a singlet in a unique manner - the wavefunction of the singlet state is particularly simple in the boson formulation:

$$\left(\varepsilon^{\alpha\beta} b_{i\alpha}^\dagger b_{j\beta}^\dagger \right)^{2S} |0\rangle \quad (100)$$

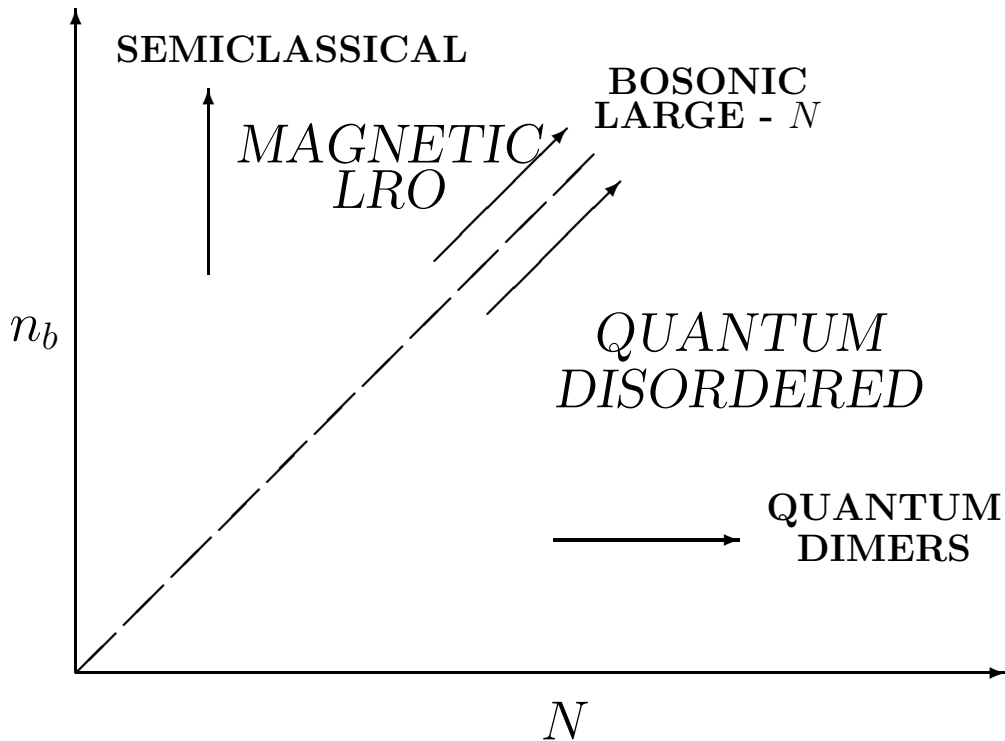


Figure 7: Phase diagram of the 2D $Sp(N)$ antiferromagnet \mathcal{H} as a function of the “spin” n_b

the “spins” on the lattice therefore belong to the symmetric product of n_b fundamentals, which is also an irreducible representation. Valence bonds

$$\mathcal{J}^{\alpha\beta} b_{i\alpha}^\dagger b_{j\beta}^\dagger \quad (106)$$

can be formed between any two sites; this operator is a singlet under $Sp(N)$ because of (104). The form (103) of \mathcal{H} has a natural generalization to general $Sp(N)$:

$$\mathcal{H} = - \sum_{i>j} \frac{J_{ij}}{2N} \left(\mathcal{J}^{\alpha\beta} b_{i\alpha}^\dagger b_{j,\beta}^\dagger \right) \left(\mathcal{J}_{\gamma\delta} b_i^\gamma b_j^\delta \right) \quad (107)$$

where the indices $\alpha, \beta, \gamma, \delta$ now run over $1 \dots 2N$. We recall also that the constraint (98) must be imposed on every site of the lattice.

We now have a two-parameter (n_b, N) family of models \mathcal{H} for a fixed realization of the J_{ij} . It is very instructive to consider the phase diagram of \mathcal{H} as a function of these two parameters (Fig. 7).

The limit of large n_b , with N fixed leads to the semi-classical theory. For the special case of $SU(2)$ antiferromagnets with a two-sublattice collinear Néel ground state, the semiclassical fluctuations are described by the $O(3)$ non-linear sigma model of Sections 3,4. For other models [26, 30, 52, 53, 54, 55, 56], the structure of the non-linear sigma models is rather more complicated and will not be considered here.

A second limit in which the problem simplifies is N large at fixed n_b [57, 26]. It can be shown that in this limit the ground state is quantum disordered. Further, the low-energy dynamics of \mathcal{H} is described by an effective quantum-dimer model [58, 26], with each dimer configuration representing a particular pairing of the sites into valence-bonds. This model is itself described by a non-trivial many-body Hamiltonian and has so far only been studied for the case of the unfrustrated square lattice antiferromagnet [59, 35, 60, 61]. We will not discuss it any further here, but existing results will be briefly noted later.

The most interesting solvable limit is obtained by fixing the ratio of n_b and N

$$\kappa = \frac{n_b}{N} \quad (108)$$

and subsequently taking the limit of large N [51]; this limit will be studied in this section in considerable detail. The implementation of \mathcal{H} in terms of bosonic operators also turns out to be naturally suited for studying this limit. The parameter κ is arbitrary; tuning κ modifies the slope of the line in Fig. 7 along which the large N limit is taken. From the previous limits discussed above, one might expect that the ground state of \mathcal{H} has magnetic LRO for large κ and is quantum-disordered for small κ . We will indeed find below that for any set of J_{ij} there is a critical value of $\kappa = \kappa_c$ which separates the magnetically ordered and the quantum disordered phase.

A powerful feature of the bosonic large- N limit noted is the existence of a second-order phase transition at $N = \infty$. In the vicinity of the phase transition, we expect the physics to be controlled by long-wavelength, low-energy spin fluctuations; the large- N method offers an unbiased guide in identifying the proper low-energy degrees of freedom and determines the effective action controlling them. Having obtained a long-wavelength continuum theory near the transition, one might hope to analyze the continuum theory independently of the large- N approximation and obtain results that are more generally valid.

We will discuss the structure of the $N = \infty$ mean-field theory, with $n_b = \kappa N$ in Section 6.A. The long-wavelength effective actions will be derived and analyzed in Section 6.B. Finally topological Berry phase effects will be considered in Section 6.C.

6.A Mean-field theory

We begin by analyzing \mathcal{H} at $N = \infty$ with $n_b = \kappa N$. As noted above, this limit is most conveniently taken using the bosonic operators. We may represent the partition function of \mathcal{H} by

$$Z = \int \mathcal{D}Q \mathcal{D}b \mathcal{D}\lambda \exp\left(-\int_0^\beta \mathcal{L} d\tau\right), \quad (109)$$

where

$$\begin{aligned} \mathcal{L} = & \sum_i \left[b_{i\alpha}^\dagger \left(\frac{d}{d\tau} + i\lambda_i \right) b_i^\alpha - i\lambda_i n_b \right] \\ & + \sum_{\langle i,j \rangle} \left[N \frac{J_{ij} |Q_{i,j}|^2}{2} - \frac{J_{ij} Q_{i,j}^*}{2} \mathcal{J}_{\alpha\beta} b_i^\alpha b_j^\beta + H.c. \right]. \end{aligned} \quad (110)$$

Here the λ_i fix the boson number of n_b at each site; τ -dependence of all fields is implicit; Q was introduced by a Hubbard-Stratonovich decoupling of \mathcal{H} . An important feature of the lagrangian \mathcal{L} is its $U(1)$ gauge invariance under which

$$\begin{aligned} b_{i\alpha}^\dagger & \rightarrow b_{i\alpha}^\dagger(i) \exp(i\rho_i(\tau)) \\ Q_{i,j} & \rightarrow Q_{i,j} \exp(-i\rho_i(\tau) - i\rho_j(\tau)) \\ \lambda_i & \rightarrow \lambda_i + \frac{\partial \rho_i}{\partial \tau}(\tau). \end{aligned} \quad (111)$$

The functional integral over \mathcal{L} faithfully represents the partition function as long as we fix a gauge, *e.g.* by the condition $d\lambda/d\tau = 0$ at all sites.

The $1/N$ expansion of the free energy can be obtained by integrating out of \mathcal{L} the $2N$ -component b, \bar{b} fields to leave an effective action for Q, λ having co-efficient N (since $n_b \propto N$). Thus the $N \rightarrow \infty$ limit is given by minimizing the effective action with respect to “mean-field” values of $Q = \bar{Q}$, $\lambda = \bar{\lambda}$ (we are ignoring here the possibility of magnetic LRO which requires an additional condensate $x^\alpha = \langle b^\alpha \rangle$ - this has been discussed elsewhere [6, 7, 8]). This is in turn equivalent to solving the mean-field Hamiltonian

$$\mathcal{H}_{MF} = \sum_{\langle i,j \rangle} \left(N \frac{J_{ij} |\bar{Q}_{ij}|^2}{2} - \frac{J_{ij} \bar{Q}_{i,j}^*}{2} \mathcal{J}_{\alpha\beta} b_i^\alpha b_j^\beta + H.c. \right) + \sum_i \bar{\lambda}_i (b_{i\alpha}^\dagger b_i^\alpha - n_b) \quad (112)$$

This Hamiltonian is quadratic in the boson operators and all its eigenvalues can be determined by a Bogouibov transformation. This leads in general to an expression of the form

$$\mathcal{H}_{MF} = E_{MF}[\bar{Q}, \bar{\lambda}] + \sum_\mu \omega_\mu[\bar{Q}, \bar{\lambda}] \gamma_{\mu\alpha}^\dagger \gamma_\mu^\alpha \quad (113)$$

The index μ extends over $1 \dots$ number of sites in the system, E_{MF} is the ground state energy and is a functional of $\bar{Q}, \bar{\lambda}$, ω_μ is the eigenspectrum of excitation energies which is also a function of $\bar{Q}, \bar{\lambda}$, and the γ_μ^α represent the bosonic eigenoperators. The excitation spectrum thus consists of non-interacting spinor bosons. The ground state is determined by minimizing E_{MF} with respect to the \bar{Q}_{ij} subject to the constraints

$$\frac{\partial E_{MF}}{\partial \bar{\lambda}_i} = 0 \quad (114)$$

The saddle-point value of the \bar{Q} satisfies

$$\bar{Q}_{ij} = \langle \mathcal{J}_{\alpha\beta} b_i^\alpha b_j^\beta \rangle \quad (115)$$

Note that $\bar{Q}_{ij} = -\bar{Q}_{ji}$ indicating that \bar{Q}_{ij} is a directed field - an orientation has to be chosen on every link.

We will now consider the ground state configurations of the \bar{Q} , $\bar{\lambda}$ fields and the nature of the bosonic eigenspectrum for a variety of non-random antiferromagnets:

6.A.1 $J_1 - J_2 - J_3$ model

This is the square lattice antiferromagnet with first (J_1), second (J_2), and third (J_3) neighbor interactions [52, 53]. We examined the values of the energy E_{MF} for \bar{Q}_{ij} configurations which had a translational symmetry with two sites per unit cell. For all parameter values configurations with a single site per unit cell were always found to be the global minima. We will therefore restrict our attention to such configurations. The $\bar{\lambda}_i$ field is therefore independent of i , while there are six independent values of \bar{Q}_{ij} :

$$\begin{aligned}
\bar{Q}_{i,i+\hat{x}} &\equiv Q_{1,x} \\
\bar{Q}_{i,i+\hat{y}} &\equiv Q_{1,y} \\
\bar{Q}_{i,i+\hat{y}+\hat{x}} &\equiv Q_{1,y+x} \\
\bar{Q}_{i,i+\hat{y}-\hat{x}} &\equiv Q_{1,y-x} \\
\bar{Q}_{i,i+2\hat{x}} &\equiv Q_{3,x} \\
\bar{Q}_{i,i+2\hat{y}} &\equiv Q_{3,y}
\end{aligned} \tag{116}$$

For this choice, the bosonic eigenstates are also eigenstates of momentum with momenta \mathbf{k} extending over the entire first Brillouin zone. The bosonic eigenenergies are given by

$$\begin{aligned}
\omega_{\mathbf{k}} &= \left(\lambda^2 - |A_{\mathbf{k}}|^2 \right)^{1/2} \\
A_{\mathbf{k}} &= J_1 (Q_{1,x} \sin k_x + Q_{1,y} \sin k_y) + J_2 (Q_{2,y+x} \sin(k_y + k_x) + Q_{2,y-x} \sin(k_y - k_x)) \\
&\quad + J_3 (Q_{3,x} \sin(2k_x) + Q_{3,y} \sin(2k_y))
\end{aligned} \tag{117}$$

We have numerically examined the global minima of E_{MF} as a function of the three parameters J_2/J_1 , J_3/J_1 , and N/n_b [6, 7]. The values of the \bar{Q}_{ij} at any point in the phase diagram can then be used to classify the distinct classes of states. The results are summarized in Figs. 8-11 which show various sections of the three-dimensional phase diagram. All of the phases are labeled by the wavevector at which the spin structure factor has a maximum. This maximum is a delta function for the phases with magnetic LRO, while it is simply a smooth function of \mathbf{k} for the quantum disordered phases (denoted by SRO in Figs 8-11). The location of this maximum will simply be twice the wavevector at which $\omega_{\mathbf{k}}$ has a minimum:

Figure 8: Ground states of the $J_1 - J_2 - J_3$ model for $J_3 = 0$ as a function of J_2/J_1 and N/n_b ($n_b = 2S$ for $SU(2)$). Thick (thin) lines denote first (second) order transitions at $N = \infty$. Phases are identified by the wavevectors at which they have magnetic long-range-order (LRO) or short-range-order (SRO). The links with $Q_p \neq 0$ in each SRO phase are shown. The large N/n_b , large J_2/J_1 phase has the two sublattices decoupled at $N = \infty$; each sublattice has Néel -type SRO. Spin-Peierls order at finite N for odd n_b is illustrated by the thick, thin and dotted lines. The (π, π) -SRO and the “decoupled” states have line-type spin-Peierls order for $n_b = 2(\text{mod } 4)$ and are valence-bond-solids for $n_b = 0(\text{mod } 4)$. The $(0, \pi)$ -SRO state is a valence-bond-solid for all even n_b .

Figure 9: As in the previous figure but as a function of J_2/J_1 and J_3/J_1 for (a) $N/n_b = 1$ and (b) $N/n_b = 5$. The inset in (a) shows the region at the tip of the arrow magnified by 20: a direct first-order transition from (π, π) -LRO to $(0, \pi)$ -LRO occurs up to $J_3/J_1 = 0.005$.

Figure 10: *As in the previous figure but for $J_3/J_1 = 0.35$*

Figure 11: *As in the previous figure but for $J_3/J_2 = 0.5$*

this is because the structure factor involves the product of two bosonic correlation functions, each of which consists of a propagator with energy denominator $\omega_{\mathbf{k}}$.

Each of the phases described below has magnetic LRO for large n_b/N and is quantum disordered for small n_b/N . The mean-field result for the structure of all of the quantum disordered phases is also quite simple: they are featureless spin fluids with free spin-1/2 bosonic excitations (“spinons”) with energy dispersion $\omega_{\mathbf{k}}$ which is gapped over the entire Brillouin zone. Notice that this result is quite different from that of the $O(M)$ non-linear sigma model of Sections 3,4 which found only integer spin excitations - the difference will be reconciled later. Some of the quantum disordered phases possess a broken lattice rotation symmetry even at $N = \infty$ - these will be described below. The minimum energy spinons lie at a wavevector \mathbf{k}_0 and $\omega_{\mathbf{k}_0}$ decreases as n_b/N . The onset of magnetic LRO occurs at the value of n_b/N at which the gap first vanishes: $\omega_{\mathbf{k}_0} = 0$. At still larger values of n_b/N , we get macroscopic bose condensation of the b quanta at the wavevector \mathbf{k}_0 , leading to magnetic LRO at the wavevector $2\mathbf{k}_0$.

We now turn to a description of the various phases obtained. They can be broadly classified into two types:

Commensurate collinear phases

In these states the wavevector \mathbf{k}_0 remains pinned at a commensurate point in the Brillouin zone, which is independent of the values of J_2/J_1 , J_3/J_1 and n_b/N . In the LRO phase the spin condensates on the sites are either parallel or anti-parallel to each other, which we identify as collinear ordering. This implies that the LRO phase remains invariant under rotations about the condensate axis and the rotation symmetry is not completely broken.

Three distinct realizations of such states were found

1. (π, π)

This is the usual two-sublattice Néel state of the unfrustrated square lattice and its quantum-disordered partner. These states have

$$Q_{1,x} = Q_{1,y} \neq 0, \quad Q_{2,y+x} = Q_{2,y-x} = Q_{3,x} = Q_{3,y} = 0 \quad (118)$$

From (117), the minimum spinon excitation occurs at $\mathbf{k}_0 = \pm(\pi/2, \pi/2)$. The SRO states have no broken symmetry at $N = \infty$. The boundary between the LRO and SRO phases occurs at $N/n_b < 2.5$, independent of J_2/J_1 (Fig 8). This last feature is surely an artifact of the large N limit. Finite N fluctuations should be stronger as J_2/J_1 increases, causing the boundary to bend a little downwards to the right.

2. $(\pi, 0)$ or $(0, \pi)$

The $(0, \pi)$ states have

$$Q_{1,x} = 0, Q_{1,y} \neq 0, Q_{2,y+x} = Q_{2,y-x} \neq 0, \text{ and } Q_{3,x} = Q_{3,y} = 0 \quad (119)$$

and minimum energy spinons at $\mathbf{k}_0 = \pm(0, \pi/2)$. The degenerate $(\pi, 0)$ state is obtained with the mapping $x \leftrightarrow y$. The SRO state has a two-field degeneracy due to the broken $x \leftrightarrow y$ lattice symmetry. The LRO state again has two-sublattice collinear Néel order, but the assignment of the sublattices is different from the (π, π) state. The spins are parallel along the x -axis, but anti-parallel along the y -axis.

An interesting feature of the LRO state here is the occurrence of order-from-disorder [62]. Recall that the classical limit ($n_b/N = \infty$) of this model has an accidental degeneracy for $J_2/J_1 > 1/2$: the ground state has independent collinear Néel order on each of the A and B sublattices, with the energy independent of the angle between the spins on the two sublattices. Quantum fluctuations are included self-consistently in the $N = \infty$, n_b/N finite, mean-field theory, and lead to an alignment of the spins on the sublattices and LRO at $(0, \pi)$. The orientation of the ground state has thus been selected by the quantum fluctuations.

The $(0, \pi)$ states are separated from the (π, π) states by a first-order transition. In particular, the spin stiffnesses of both states remain finite at the boundary between them. This should be distinguished from the classical limit in which the stiffness of both states vanish at their boundary $J_2 = J_1/2$; the finite spin stiffnesses are thus another manifestation of order-from-disorder. At a point well away from the singular point $J_2 = J_1/2$, $n_b/N = \infty$ in Fig 8, the stiffness of both states is of order $N(n_b/N)^2$ for $N = \infty$ and large n_b/N ; near this singular point however the stiffness is of order $N(n_b/N)$ is induced purely by quantum fluctuations. These results have since also been obtained by a careful resummation of the semiclassical expansion [63, 64].

3. “Decoupled”

For J_2/J_1 and N/n_b both large, we have a “decoupled” state (Fig 8) with

$$Q_{2,y+x} = Q_{2,y-x} \neq 0 \text{ and } Q_1 = Q_3 = 0. \quad (120)$$

In this case Q_p is non-zero only between sites on the same sublattice. The two sublattices have Néel type SRO which will be coupled by finite N fluctuations. The $N = \infty$ state does not break any lattice symmetry. This state has no LRO partner.

Incommensurate phases

In these phases the wavevector \mathbf{k}_0 and the location of the maximum in the structure factor move continuously with the parameters [65]. The spin-condensate rotates with a period which is not commensurate with the underlying lattice spacing. Further the spin condensate is *coplanar*: the spins rotate within a given plane in spin space and are not collinear. There is this no spin rotation axis about which the LRO state remains invariant.

Further, no states in which the spin condensate was fully three dimensional (“double-spiral” or chiral states) were found; these would be associated with complex values of Q_p . All the saddle points possessed a gauge in which all the Q_p were real. Time-reversal symmetry was therefore always preserved in all the SRO phases of Figs 8-11.

The incommensurate phases occur only in models with a finite J_3 (Figs 9-11). There were two realizations:

1. (π, q) or (q, π)

Here q denotes a wavevector which varies continuously between 0 and π as the parameters are changed. The (q, π) state has

$$Q_{1,x} \neq Q_{1,y} \neq 0, \quad Q_{2,x+y} = Q_{2,y-x} \neq 0, \quad Q_{3,x} \neq 0 \text{ and } Q_{3,y} = 0; \quad (121)$$

the degenerate (π, q) helix is obtained by the mapping $x \leftrightarrow y$. The SRO state has a two-fold degeneracy due to the broken $x \leftrightarrow y$ lattice symmetry.

2. (q, q) or $(q, -q)$

The (q, q) state has

$$Q_{1,x} = Q_{1,y} \neq 0, \quad Q_{2,x+y} \neq 0, \quad Q_{2,y-x} = 0, \quad Q_{3,x} = Q_{3,y} \neq 0; \quad (122)$$

this is degenerate with the $(q, -q)$ phase and SRO state therefore has a two-fold degeneracy due to a broken lattice reflection symmetry.

Note that the broken discrete symmetries in states with SRO at $(0, \pi)$ and (q, π) are identical: both are two-fold degenerate due to a breaking of the $x \leftrightarrow y$ symmetry. The states are only distinguished by a non-zero value of Q_3 in the (q, π) phase and the accompanying incommensurate correlations in the spin-spin correlation functions. However Q_3 is gauge-dependent and so somewhat unphysical as an order parameter. In the absence of any further fluctuation-driven lattice symmetry breaking (see below), the transition between SRO at $(0, \pi)$ and (q, π) is an example of a *disorder line* [66]; these are lines at which incommensurate correlations first turn on.

An interesting feature of Figs 10-11 is that the commensurate states squeeze out the incommensurate phases as N/n_b increases in both phase diagrams. We expect that this suppression of incommensurate order by quantum fluctuations is a general feature of frustrated antiferromagnets. This result is also consistent with the natural hypothesis that the states of the large N , fixed, but small n_b/N should be consistent with the states of the large N , fixed n_b theory (Fig. 7). This latter limit is described by the quantum-dimer model [58] which is necessarily associated only with commensurate states.

6.A.2 Triangular and Kagomé Lattices

We have also examined the mean-field equations for the nearest-neighbor antiferromagnet on the triangular [67] and kagomé lattices in considerable detail [8]. In both cases we found that the SRO phases had the *full symmetry of the underlying lattice*. They differ in this manner from all of the SRO phases of the square lattice. Further the \bar{Q}_{ij} were real on every link and had the same magnitude $|\bar{Q}_{ij}| = Q$. The only remaining degree of freedom is that associated with assigning an orientation to each link: minimization of the energy determined a unique orientation upto gauge-equivalent configurations.

On the triangular lattice the spectrum of the free spin-1/2 bosonic spinon excitations was found to be given by

$$\omega(\mathbf{k}) = \left(\lambda^2 - J^2 Q^2 (\sin k_1 + \sin k_2 + \sin k_3)^2 \right)^{1/2} \quad (123)$$

where the momentum \mathbf{k} ranges over the first Brillouin zone of the triangular lattice and

$$k_p = \mathbf{k} \cdot \hat{e}_p \quad (124)$$

with the \hat{e}_p being unit vectors of length a pointing along the directions of the bonds on the triangular lattice

$$\begin{aligned} \hat{e}_1 &= a(1/2, \sqrt{3}/2) \\ \hat{e}_2 &= a(1/2, -\sqrt{3}/2) \\ \hat{e}_3 &= a(-1, 0) \end{aligned} \quad (125)$$

A surface plot of this spectrum is shown in Fig 12 for $n_b/N = 0.25$. The minimum-energy spinons are those at $\mathbf{k}_{01} = (4\pi/3a)(1, 0)$ and $\mathbf{k}_{02} = (4\pi/3a)(-1, 0)$ and other points separated from these points by vectors of the reciprocal lattice generated by $\mathbf{G}_1 = (4\pi/\sqrt{3}a)(0, 1)$ and $\mathbf{G}_2 = (4\pi/\sqrt{3}a)(\sqrt{3}/2, -1/2)$. For $n_b/N > 0.34$ this state acquires magnetic LRO with the conventional three-sublattice Néel ordering of the triangular lattice. The spins are *coplanar* pointing towards the vertices of an equilateral triangle.

Figure 12: Momentum dependence of the energy, $\omega(\mathbf{k})$ of the lowest excited spinon state for the quantum-disordered ground state of the triangular lattice quantum antiferromagnet at $\kappa = 0.25$. The minimum excitations are the spinons at $\mathbf{k} = \tilde{\mathbf{k}}_1 = (4\pi/3a)(1, 0)$ and $\mathbf{k} = \tilde{\mathbf{k}}_2 = (4\pi/3a)(-1, 0)$ and other points separated from $\tilde{\mathbf{k}}_1, \tilde{\mathbf{k}}_2$ by vectors of the reciprocal lattice

Very similar results were obtained on the kagomé lattice. As this is not a Bravais lattice, it is necessary to introduce three sites per unit cell although no symmetry of the lattice is broken by the SRO state. To determine the free spin-1/2 bosonic excitation spectrum we need the following matrix

$$P(\mathbf{k}) = -iJQ \begin{pmatrix} 0 & \sin k_1 & \sin k_3 \\ \sin k_1 & 0 & \sin k_2 \\ \sin k_3 & \sin k_2 & 0 \end{pmatrix}. \quad (126)$$

(the k_p were defined in Eqs. (124) and (125)) and to solve the eigenvalue equation

$$P^\dagger(\mathbf{k})P(\mathbf{k})\varphi_\mu(\mathbf{k}) = p_\mu^2(\mathbf{k})\varphi_\mu(\mathbf{k}) \quad (127)$$

where p_μ^2 , $\mu = 1, 2, 3$ are the eigenvalues and $\varphi_\mu(\mathbf{k})$ the eigenvectors. Finally the bosonic eigenspectrum is given by

$$\omega_\mu(\mathbf{k}) = (\lambda^2 - p_\mu^2(\mathbf{k}))^{1/2} \quad (128)$$

The lowest energy spinon spectrum for $n_b/N = 0.35$ is plotted in Fig 13. The minimum energy spinons are at $\mathbf{k} = \mathbf{k}_1 = (2\pi/3a)(1, 0)$ and $\mathbf{k} = \mathbf{k}_2 = (2\pi/3a)(-1, 0)$ and other points separated from $\mathbf{k}_1, \mathbf{k}_2$ by vectors of the reciprocal lattice generated by $\mathbf{G}_1 = (2\pi/\sqrt{3}a)(0, 1)$ and $\mathbf{G}_2 = (2\pi/\sqrt{3}a)(\sqrt{3}/2, -1/2)$. There is no quite good evidence that the spin-1/2, nearest-neighbor, kagomé antiferromagnet is quantum disordered [68, 69]. The present calculation should therefore be relevant for this system.

The spinon gap vanishes and magnetic LRO appears for $n_b/N > 0.53$. The magnetic LRO is the configuration identified as the coplanar “ $\sqrt{3} \times \sqrt{3}$ ” structure in the literature [70, 71, 72, 73]. The huge accidental degeneracy of the classical ground state on the kagomé lattice is completely lifted by the quantum fluctuations, and unique (upto global spin rotations) magnetic structure is obtained as the ground state. Note the rather natural way in which this happened directly in the the mean-field theory. The present large- N approach thus seems to be ideally suited to examining order-from-disorder issues in frustrated antiferromagnets.

6.B Fluctuations - long wavelength effective actions

We now extend the analysis of Section 6.B beyond the mean-field theory and examine the consequences of corrections at finite N . The main question we hope to address are:

- The mean-field theory yielded an excitation spectrum consisting of free spin-1/2 bosonic spinons. We now want to understand the nature of the forces between these spinons and whether they can lead to confinement of half-integer spin excitations.
- Are there any collective excitations and does their dynamics modify in any way the nature of the ground state ?

Figure 13: Momentum dependence of the energy, $\omega(\mathbf{k})$ of the lowest excited spinon state for the quantum-disordered ground state (which has $Q_1 = -Q_2$) of the kagomé lattice quantum antiferromagnet at $\kappa = 0.35$. The energy is measured in units of $J/2$, and a is the nearest-neighbor spacing on the kagomé lattice. The minimum excitations are the spinons at $\mathbf{k} = \mathbf{k}_1 = (2\pi/3a)(1, 0)$ and $\mathbf{k} = \mathbf{k}_2 = (2\pi/3a)(-1, 0)$ and other points separated from $\mathbf{k}_1, \mathbf{k}_2$ by vectors of the reciprocal lattice

The structure of the fluctuations will clearly be determined by the low-energy excitations about the mean-field state. We have already identified one set of such excitations: spinons at momenta near minima in their dispersion spectrum, close to the onset of the magnetic LRO phase whence the spinon gap vanishes. An additional set of low-lying spinless excitations can arise from the fluctuations of the Q_{ij} and λ_i fields about their mean-field values. The gauge-invariance (111) will act as a powerful restriction on the allowed in the effective action for these spinless fields. We anticipate that the only such low-lying excitations are associated with the λ_i and the *phases* of the Q_{ij} . We therefore parametrize

$$Q_{i,i+\hat{e}_p} = \bar{Q}_{i,i+\hat{e}_p} \exp(-i\Theta_p) \quad (129)$$

where the vector \hat{e}_p connects the two sites of the lattice under consideration, \bar{Q} is the mean-field value, and Θ_p is a real phase. The gauge invariance (111) implies that the effective action for the Θ_p must be invariant under

$$\Theta_p \rightarrow \Theta_p + \rho_i + \rho_{i+\hat{e}_p}. \quad (130)$$

Upon performing a Fourier transform, with the link variables Θ_p placed on the center of the links, the gauge invariance takes the form

$$\Theta_p(\mathbf{k}) \rightarrow \Theta_p(\mathbf{k}) + 2\rho(\mathbf{k}) \cos(k_p/2) \quad (131)$$

where $k_p = \mathbf{k} \cdot \hat{e}_p$. This invariance implies that the effective action for the Θ_p , after integrating out the b quanta, can only be a function of the following gauge-invariant combinations:

$$I_{pq} = 2 \cos(k_q/2) \Theta_p(\mathbf{k}) - 2 \cos(k_p/2) \Theta_q(\mathbf{k}) \quad (132)$$

We now wish to take the continuum limit at points in the Brillouin zone where the action involves only gradients of the Θ_p fields and thus has the possibility of gapless excitations. This involves expanding about points in the Brillouin zone where

$$\cos(k_p/2) = 0 \text{ for the largest numbers of } \hat{e}_p \quad (133)$$

We will apply this general principle to the models considered in Sec. 6.A.

6.B.1 $J_1 - J_2 - J_3$ Model

We begin by examining the (π, π) -SRO phase. As noted in (118), this phase has the mean field values $Q_{1,x} = Q_{1,y} \neq 0$, and all other \bar{Q}_{ij} zero. Thus we need only examine the condition (133) with $\hat{e}_p = \hat{e}_x, \hat{e}_y$. This uniquely identifies the point $\mathbf{k} = \mathbf{G} = (\pi, \pi)$ in the Brillouin zone. We therefore parametrize

$$\Theta_x(\mathbf{r}) = i e^{i\mathbf{G} \cdot \mathbf{r}} A_x(\mathbf{r}) \quad (134)$$

and similarly for Θ_y ; it can be verified that both Θ and A_x are real in the above equation. We will also be examining invariances of the theory under gauge transformations near \mathbf{G} : so we write

$$\rho(\mathbf{r}) = e^{i\mathbf{G}\cdot\mathbf{r}}\varphi(\mathbf{r}) \quad (135)$$

It is now straightforward to verify that the gauge transformations (131) are equivalent to

$$A_x \rightarrow A_x + \partial_x\varphi \quad (136)$$

and similarly for A_y . We will also need in the continuum limit the component of λ near the wavevector \mathbf{G} . We therefore write

$$\lambda_i = \bar{\lambda} + ie^{i\mathbf{G}\cdot\mathbf{r}}A_\tau(\mathbf{r}_i) \quad (137)$$

Under gauge transformations we have

$$A_\tau \rightarrow A_\tau + \partial_\tau\varphi \quad (138)$$

Thus A_x, A_y, A_τ transform as components of a continuum $U(1)$ vector gauge field.

We will also need the properties of the boson operators under φ . From (111) and (135) we see that the bosons on the two sublattices (A, B) with opposite charges ± 1 :

$$\begin{aligned} b_A &\rightarrow b_A e^{i\varphi} \\ b_B &\rightarrow b_B e^{-i\varphi} \end{aligned} \quad (139)$$

Finally, we note that the bosonic eigenspectrum has a minimum near $\mathbf{k} = \mathbf{k}_0 = (\pi/2, \pi/2)$; we therefore parametrize

$$\begin{aligned} b_{Ai}^\alpha &= \psi_1^\alpha(\mathbf{r}_i) e^{i\mathbf{k}_0\cdot\mathbf{r}_i} \\ b_{Bi}^\alpha &= -i\mathcal{J}^{\alpha\beta}\psi_{1\beta}(\mathbf{r}_i) e^{i\mathbf{k}_0\cdot\mathbf{r}_i} \end{aligned} \quad (140)$$

We insert the continuum parametrizations (134), (137) and (140) into the functional integral (110), perform a gradient expansion, and transform the Lagrangian \mathcal{L} into

$$\begin{aligned} \mathcal{L} = \int \frac{d^2r}{a^2} &\left[\psi_{1\alpha}^* \left(\frac{d}{d\tau} + iA_\tau \right) \psi_1^\alpha + \psi_2^{\alpha*} \left(\frac{d}{d\tau} - iA_\tau \right) \psi_{2\alpha} + \bar{\lambda} (|\psi_1^\alpha|^2 + |\psi_{2\alpha}|^2) \right. \\ &- 4J_1\bar{Q}_1 (\psi_1^\alpha\psi_{2\alpha} + \psi_{1\alpha}^*\psi_2^{\alpha*}) + J_1\bar{Q}_1 a^2 \left[(\vec{\nabla} + i\vec{A}) \psi_1^\alpha (\vec{\nabla} - i\vec{A}) \psi_{2\alpha} \right. \\ &\left. \left. + (\vec{\nabla} - i\vec{A}) \psi_{1\alpha}^* (\vec{\nabla} + i\vec{A}) \psi_2^{\alpha*} \right] \right] \quad (141) \end{aligned}$$

We now introduce the fields

$$\begin{aligned} z^\alpha &= (\psi_1^\alpha + \psi_2^{\alpha*})/\sqrt{2} \\ \pi^\alpha &= (\psi_1^\alpha - \psi_2^{\alpha*})/\sqrt{2}. \end{aligned}$$

From Eqn (141), it is clear that the the π fields turn out to have mass $\bar{\lambda} + 4J_1\bar{Q}_1$, while the z fields have a mass $\bar{\lambda} - 4J_1\bar{Q}_1$ which vanishes at the transition to the LRO phase. The π fields can therefore be safely integrated out, and \mathcal{L} yields the following effective action, valid at distances much larger than the lattice spacing [34, 35]:

$$S_{eff} = \int \frac{d^2r}{\sqrt{8a}} \int_0^{c\beta} d\tilde{\tau} \left\{ |(\partial_\mu - iA_\mu)z^\alpha|^2 + \frac{\Delta^2}{c^2}|z^\alpha|^2 \right\}, \quad (142)$$

Here μ extends over x, y, z , $c = \sqrt{8}J_1\bar{Q}_1a$ is the spin-wave velocity, $\Delta = (\lambda^2 - 16J_1^2\bar{Q}_1^2)^{1/2}$ is the gap towards spinon excitations, and $A_{\tilde{\tau}} = A_\tau/c$. Thus, in its final form, the long-wavelength theory consists of a massive, spin-1/2, relativistic, boson z^α (spinon) coupled to a compact $U(1)$ gauge field.

At distances larger than c/Δ , we may safely integrate out the massive z quanta and obtain a compact $U(1)$ gauge theory in 2+1 dimensions. This theory was argued by Polyakov [36, 74] to be permanently in a confining phase, with the confinement driven by ‘‘instanton’’ tunnelling events. The compact $U(1)$ gauge force will therefore confine the z^α quanta in pairs. In the present theory, the confinement length scale turns out to be exponentially large in N : $\sim e^{cN}$ where the constant c diverges logarithmically as $\Delta \rightarrow 0$ [46]. There are thus no free spin-1/2 bosonic excitations for any finite N and all low-lying modes carry integral spin. The presence of an unbroken $U(1)$ gauge force in the fluctuations has therefore completely disrupted the simple mean-field structure of these states. The spectrum of the A_μ quanta also acquires a gap from instantons effects which is exponentially small in N [74, 46].

The properties of the $(0, \pi)$ phase are very similar to those of the (π, π) phase considered above, and will therefore not be discussed here. It can be shown quite generally that any quantum disordered state which has appreciable commensurate, collinear spin correlations will have similar properties: confined spinons and a collective mode described by a compact $U(1)$ gauge theory.

We now turn to a study of the incommensurate phases. It is not difficult to show that in this case it is not possible to satisfy the constraints (133) at any point in the Brillouin zone for all the non-zero Q_p . This implies that there is no gapless collective mode in the incommensurate SRO phases. The structure of the theory is simplest in the vicinity of a transition to a commensurate collinear phase: we now examine the effective action as one

moves from the (π, π) -SRO phase into the (q, q) -SRO phase (Figs 10-11) (a very similar analysis can be performed at the boundary between the (π, π) -SRO and the (π, q) -SRO phases). This transition is characterized by a continuous turning on of non-zero values of $Q_{i, i+\hat{y}+\hat{x}}$, $Q_{i, i+2\hat{x}}$ and $Q_{i, i+2\hat{y}}$. It is easy to see from Eqn (111) that these fields transform as scalars of charge ± 2 under the gauge transformation associated with A_μ . Performing a gradient expansion upon the bosonic fields coupled to these scalars we find that the Lagrangian \mathcal{L} of the (π, π) -SRO phase gets modified to

$$\mathcal{L} \rightarrow \mathcal{L} + \int \frac{d^2 r}{a} \left(\vec{\Phi}_A \cdot \left(\mathcal{J}_{\alpha\beta} \psi_1^\alpha \vec{\nabla} \psi_1^\beta \right) + \vec{\Phi}_B \cdot \left(\mathcal{J}^{\alpha\beta} \psi_{2\alpha} \vec{\nabla} \psi_{2\beta} \right) + \text{c.c.} \right) \quad (143)$$

where $\vec{\Phi}_{A,B}$ are two-component scalars $\equiv (J_3 Q_{3,x} + J_2 Q_{2,y+x}, J_3 Q_{3,y} + J_2 Q_{2,y+x})$ with the sites on the ends of the link variables on sublattices A, B . Finally, as before, we transform to the z, π variables, integrate out the π fluctuations and obtain [7]

$$S_{eff} = \int \frac{d^2 r}{\sqrt{8}a} \int_0^{c\beta} d\tilde{\tau} \left\{ |(\partial_\mu - iA_\mu)z^\alpha|^2 + r|z^\alpha|^2 + \vec{\Phi} \cdot \left(\mathcal{J}_{\alpha\beta} z^\alpha \vec{\nabla} z^\beta \right) + \text{c.c.} + V(\Phi) \right\} + \dots, \quad (144)$$

Here $r = \Delta^2/c^2$, $\vec{\Phi} = (\vec{\Phi}_A + \vec{\Phi}_B^*)/(2J_1\bar{Q}_1a)$ is a scalar of charge -2 ; terms higher order in $\vec{\Phi}$ have been dropped. We have also added a phenomenological potential $V(\Phi)$ which is generated by short wavelength fluctuations of the b^α quanta. This effective action is also the simplest theory that can be written down which couples a spin-1/2, charge 1, boson z^α , a compact $U(1)$ gauge field A_μ , and a two spatial component, charge -2 , spinless boson $\vec{\Phi}$. It is the main result of this section and summarizes essentially all of the physics we are trying to describe. We now describe the various phases of S_{eff}

1. Commensurate, collinear, LRO: $\langle z^\alpha \rangle \neq 0$, $\langle \vec{\Phi} \rangle = 0$

This is the state with commensurate, collinear, magnetic LRO

2. Commensurate, collinear, SRO: $\langle z^\alpha \rangle = 0$, $\langle \vec{\Phi} \rangle = 0$

This is the quantum-disordered state with collinear spin correlations peaked at (π, π) . Its properties were described at length above. The compact $U(1)$ gauge force confines the z^α quanta. The spinless collective mode associated with the gauge fluctuations also has a gap.

3. Incommensurate, coplanar, SRO: $\langle z^\alpha \rangle = 0$, $\langle \vec{\Phi} \rangle \neq 0$

This is the incommensurate phase with SRO at (q, q) which we want to study. It is easy to see that condensation of $\vec{\Phi}$ necessarily implies the appearance of incommensurate SRO: ignore fluctuations of $\vec{\Phi}$ about $\langle \vec{\Phi} \rangle$ and diagonalize the quadratic form controlling

the z^α fluctuations; the minimum of the dispersion of the z^α quanta is at a non-zero wavevector

$$\mathbf{k}_0 = (\langle \Phi_x \rangle, \langle \Phi_y \rangle) / 2 \quad (145)$$

The spin structure factor will therefore have a maximum at an incommensurate wavevector. This phase also has a broken lattice rotation symmetry due to the choice of orientation in the $x - y$ plane made by $\vec{\Phi}$ condensate. The condensation of $\vec{\Phi}$ also has a dramatic impact on the nature of the force between the massive z^α quanta. Detailed arguments have been presented by Fradkin and Shenker [75] that the condensation of a doubly charged Higgs scalar quenches the confining compact $U(1)$ gauge force in 2+1 dimensions between singly charged particles. Applied to the present problem, this implies that the charge -2 field $\vec{\Phi}$ condenses and deconfines the z^α quanta. The excitation structure is therefore very similar to that of the mean-field theory: spin-1/2, massive bosonic spinons and spinless collective modes which have a gap. The collective mode gap is present in this case even at $N = \infty$ and is associated with the condensation of $\vec{\Phi}$.

4. Incommensurate, coplanar, LRO: $\langle z^\alpha \rangle \neq 0$, $\langle \vec{\Phi} \rangle \neq 0$

The condensation of the z quanta at the wavevector \mathbf{k}_0 above leads to incommensurate LRO, with the spin condensate spiraling in the plane.

6.B.2 Triangular and Kagomé Lattices

We will focus mainly on the nature of the fluctuations on the triangular lattice [8]. The properties of the kagomé lattice are very similar and have been discussed elsewhere [8].

The magnetically ordered state on the triangular lattice is coplanar. From the results on the $J_1 - J_2 - J_3$ model we anticipate that the fluctuations about the quantum disordered state on the triangular lattice will be similar to those of the incommensurate, coplanar, SRO states - there will be no gapless gauge modes and the spin-1/2 spinons remain unconfined.

We now present a few details verifying this conjecture. It is not difficult to see that the constraint (133) for low-lying gauge modes can be satisfied at most two of the values of $p = 1, 2, 3$ (corresponding to the \hat{e}_p in Eqns. (125)) at any point of the Brillouin zone. One such point is the wavevector

$$\mathbf{g}_a = \frac{2\pi}{\sqrt{3}a}(0, 1) \quad (146)$$

where

$$g_{a1} = \pi$$

$$\begin{aligned}
g_{a2} &= -\pi \\
g_{a3} &= 0
\end{aligned}
\tag{147}$$

Taking the continuum limit with the fields varying with momenta with close to \mathbf{g}_a we find that the I_{pq} in (132) depend only upon gradients of Θ_1 and Θ_2 . Under gauge transformations near the momentum \mathbf{g}_a , the bosons

$$b_i^\alpha \text{ carry charges } \exp(i\mathbf{g}_a \cdot \mathbf{r}_i). \tag{148}$$

It can be verified that these charges only take the values ± 1 on the lattice sites. We have therefore imposed a certain ‘staggering’ of the charge assignments of the bosons which is quite analogous to that in the square-lattice antiferromagnets in Sec. 6.B.1. It is also helpful to parametrize the Θ_p in the following suggestive manner

$$\begin{aligned}
\Theta_1(\mathbf{r}) &= iA_{a1}(\mathbf{r})e^{i\mathbf{g}_a \cdot \mathbf{r}} \\
\Theta_2(\mathbf{r}) &= -iA_{a2}(\mathbf{r})e^{i\mathbf{g}_a \cdot \mathbf{r}} \\
\Theta_3(\mathbf{r}) &= \Phi_a(\mathbf{r})e^{i\mathbf{g}_a \cdot \mathbf{r}}
\end{aligned}
\tag{149}$$

It can be verified that the condition for the reality of Θ_p is equivalent to demanding that A_{a1}, A_{a2}, Φ_a be real. We will now take the continuum limit with A_{a1}, A_{a2}, Φ_a varying slowly on the scale of the lattice spacing. It is then not difficult to show that the invariants I_{pq} then reduce to (after a Fourier transformation):

$$\begin{aligned}
I_{12} &= \hat{e}_2 \cdot \vec{\nabla} A_{a1} - \hat{e}_1 \cdot \vec{\nabla} A_{a2} \\
I_{31} &= \hat{e}_1 \cdot \vec{\nabla} \Phi_a - 2A_{a1} \\
I_{32} &= \hat{e}_2 \cdot \vec{\nabla} \Phi_a - 2A_{a2}
\end{aligned}
\tag{150}$$

Thus the A_{a1}, A_{a2} are the components of the connection of a gauge symmetry denoted $U_a(1)$; the components are taken along an ‘oblique’ co-ordinate system defined by the axes \hat{e}_1, \hat{e}_2 . The field Φ_a transforms as the phase of charge 2 Higgs field under $U_a(1)$.

A very similar analysis can be carried out near the two other points in the Brillouin zone where the other pairs of values of $\cos(k_p/2)$ vanish. These are the points

$$\begin{aligned}
\mathbf{g}_b &= \frac{2\pi}{\sqrt{3}a} \left(\frac{\sqrt{3}}{2}, -\frac{1}{2} \right) \\
\mathbf{g}_c &= \frac{2\pi}{\sqrt{3}a} \left(\frac{-\sqrt{3}}{2}, -\frac{1}{2} \right)
\end{aligned}
\tag{151}$$

which introduce the continuum symmetries $U_b(1)$ and $U_c(1)$ respectively. The Θ_p now reduce in the continuum limit to fields Φ_b, A_{b2}, A_{b3} and A_{c1}, Φ_c, A_{c3} respectively. Thus in the continuum limit the lattice $U(1)$ gauge symmetry has been replaced by a $U_a(1) \times U_b(1) \times U_c(1)$

gauge symmetry. The three gauge symmetries correspond to the three different ways the triangular lattice can be distorted into a rectangular lattice with diagonal bonds: the phases on the horizontal and vertical bonds behave like gauge connections while the phases on the diagonal bonds become charge 2 Higgs fields. The system also possesses spin-1/2 boson excitations which carry charges ± 1 of all 3 symmetries.

The condensation of all of the Higgs fields is implicit, and there are therefore no low-lying physical gauge excitations. As in Sec. 6.B.1, we conclude that the instantons are quenched and that unit charges are expected to be unconfined [75]; in particular the spin-1/2 boson quanta, which carry the $U_a(1)$ charges specified in (148), and analogous $U_b(1)$ and $U_c(1)$ charges, will remain unconfined.

6.C Berry Phases

We found two different radically different consequences of gauge fluctuations in the quantum-disordered phases in section 6.B:

- (a) the commensurate collinear phases appeared to have gapless gauge modes; however, they acquired a gap from instanton effects which also led to the confinement of spinons.
- (b) the coplanar phases on the square, triangular, and kagomé phases had only gapped gauge fluctuations; the mean-field spectrum was stable to fluctuation effects and the bosonic spinons remained unconfined.

It was also clear from the analyses in Sections 6.B and 3 that the Berry phases of small fluctuations about the mean-field saddle points had been properly accounted for.

The only possibility that has not been explored carefully is that the topologically non-trivial gauge field configurations (instantons, vortices) might possess some non-trivial Berry phases. Such phases are of course not present in a theory with a simple Maxwell action for the gauge-field fluctuations; in the present theory the effective action is much more complicated and the bosons propagate in a complicated gauge-field background can acquire Berry phases. Such effects can, in principle, be present in both the collinear and coplanar SRO phases. However, in the vicinity of the transition to the LRO phases, instanton effects are not expected to be dominant in the coplanar states; in contrast the collinear phases have already been shown to be radically modified by instanton effects.

Detailed calculations of instanton Berry phase effects have been performed in the collinear phases. These calculations are rather involved and the reader is referred to Ref. [35] for further details: we will simply present the results here. It was first shown by Haldane [33], using the non-linear sigma model formulation of Section 3 for fluctuations in the (π, π) LRO

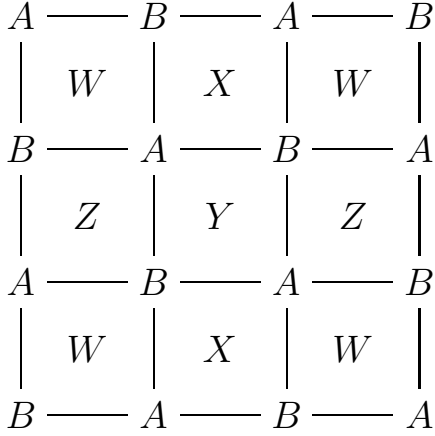


Figure 14: The A, B sublattices of the lattice of spins and the sublattices W, X, Y, Z of the dual lattice.

state, that ‘hedgehog’ \mathbf{n} configurations had the following Berry phase term in its action

$$S_B = i \frac{\pi n_b}{2} \sum_s m_s \zeta_s \quad (152)$$

where $n_b = 2S$, m_s is the charge of an hedgehog centered on the square lattice plaquette numbered s , and ζ_s takes the values 0, 1, 2, 3 on the W, X, Y, Z plaquette sublattices (Fig 14); it can be shown that no symmetry is broken by this choice of phases, and that all observable correlation functions are invariant under the full lattice symmetry group (in the absence of any dynamical symmetry breaking, of course). Note that this phase is always unity for even-integer spins.

Subsequently, Refs [34, 35] examined these Berry phases directly in the commensurate, collinear SRO phases. It was argued that the remnants of the hedgehogs in the LRO phases were precisely the instantons in the compact $U(1)$ gauge field of Section 6.B. The Berry phase of bosons propagating in an instanton gauge-field background was evaluated and found to be identical to (152) in the (π, π) SRO phase; m_s is now the total flux emanating from the instanton divided by 2π . The result in the $(0, \pi)$ SRO phase was different [7]:

$$S_B = i\pi n_b \sum_s m_s [R_{sx}] \quad (153)$$

where $[R_{sx}]$ is the integer part of R_x , the x -coordinate of the plaquette s ; this phase is unity for all integer spins. The result in the decoupled state was imply two copies of the (π, π) SRO phase.

An analysis of the dynamics of the instantons was then carried out [34, 76]. In the SRO phase the instantons interact with a Coulombic $1/R$ potential; the instanton plasma can

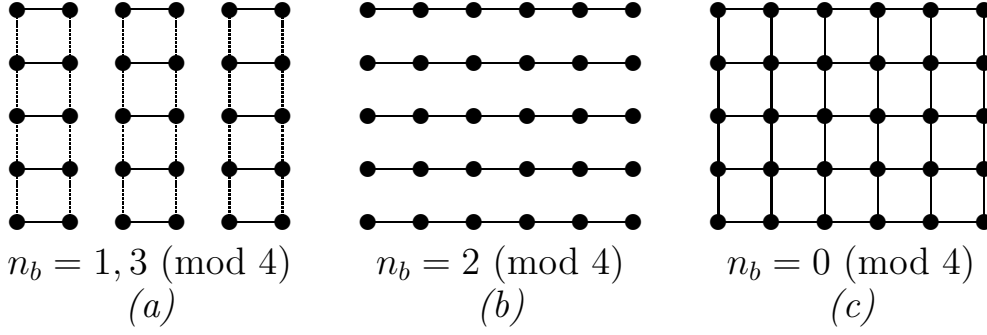


Figure 15: Symmetry of non-Néel ground states of H as a function of $n_b \pmod{4}$ with the minimum possible degeneracies of 4,2,1 respectively ($n_b = 2S$ for $SU(2)$). The full-dotted-blank lines represent different values of $\langle \hat{\mathbf{S}}_i \cdot \hat{\mathbf{S}}_j \rangle$ on the links.

therefore be mapped onto a dual sine-Gordon model in which the instanton Berry phases appear as frustrating phase-shifts in the arguments of the cosine term. Finally analysis of this sine-Gordon model showed that non-unity Berry phases led to spontaneous breaking of a lattice rotational symmetry through the appearance of spin-Peierls order. The nature of the spin-Peierls ordering depended strongly on the value of $n_b \pmod{4}$.

For the case of (π, π) SRO the spin-Peierls ordering is shown in Fig 15. The valence-bonds align in columns (4-fold degenerate) for half-integer spins, and along lines (2-fold degenerate) for integer spins. Only for even integer spins is there no breaking of symmetry and we obtain a valence-bond-solid state [50]. It is interesting that an analysis of the quantum-dimer model [59] for $n_b = 1$ also found spin-Peierls order of the columnar type. Thus the $N \rightarrow \infty$, $n_b = 1$ theory agrees with the $N \rightarrow \infty$, n_b/N fixed, $n_b = 1 \pmod{4}$ theory.

In the “decoupled” SRO phase, the above analysis applies to each sublattice separately, giving for $n_b = 1 \pmod{4}$ the type of spin-Peierls correlations shown in Fig 8. There is a total of $4 \times 4 = 16$ states for this case but coupling between the sublattices will reduce this to 8 states, all of one of the two types shown. The state with the ‘dimers’ parallel to one another has more possibilities for resonance using the J_1 bonds and is likely to be the ground state. For $n_b = 2 \pmod{4}$, there will be $2 \times 2/2 = 2$ states, and for $n_b = 0 \pmod{4}$, just one.

For the $(0, \pi)$ SRO state the spin-Peierls order of the type shown in Fig 8 for n_b odd (half-integer spins), and a VBS state for n_b even (integer spins). Combined with the choice $(0, \pi)$ or $(\pi, 0)$ this gives degeneracies 2, 4, 2, 4 for $n_b = 0, 1, 2, 3 \pmod{4}$.

6.D Summary

The above analysis has been rather involved, but the essential results are rather simple. Let us recall here the main properties of the quantum disordered phases found in two dimensional antiferromagnets.

- Commensurate, collinear phases

The spin structure factor has a well-defined maximum at a commensurate point in the Brillouin zone. The spinon excitations are massive and confined in pairs - there are no low-lying excitations with half-integral spins. There is a spinless collective mode which has a gap induced by instanton effects. Spin-Peierls order is present and its nature depends on the value of $n_b \pmod{4}$ (for the square lattice).

- Incommensurate, coplanar phases

The spin structure factor has well-defined maxima at incommensurate points in the Brillouin zone. The spin-1/2 spinon excitations are massive, deconfined and carry bosonic statistics. The spinless collective mode has a gap induced by the condensation of a Higgs field: the magnitude of the condensate is proportional to the incommensuration. There is a broken lattice reflection symmetry associated with the choice of an axis about which the fluctuating spiral order is present.

- Commensurate, coplanar fluids on the triangular and kagomé lattices

These phases form the incommensurate coplanar states only in that the peak of the structure factor is at a commensurate point, and there is no broken symmetry. These states thus appear to violate Laughlin's fractional quantization principle [77] that all spin-1/2 excitations of featureless spin-fluids should possess fractional statistics: the spinons in the present theory are bosonic.

6. Comparison with numerical and series results

Many numerical [78] and series analyses [79] have appeared on the $J_1 - J_2 - J_3$ model with $J_3 = 0$ for the spin-1/2 $SU(2)$ model *i.e.* $N = 1$, $n_b = 1$ in the notation of this paper. They find (π, π) -LRO at small J_2/J_1 , $(\pi, 0)$ -LRO at large J_2/J_1 and an intermediate SRO phase around $J_2/J_1 = 1/2$. This is in agreement (see Fig 8) with our prediction in Section 6.B that the phase boundary between (π, π) -LRO and (π, π) -SRO bends downwards at finite N with increasing J_2/J_1 . Analyses of this intermediate phase at J_2/J_1 [78, 79] shows clear evidence of columnar spin-Peierls ordering [34], also in agreement with the results of Section 6.C. An additional intermediate phase with $(0, \pi)$ -SRO has not been ruled out.

There has also been intensive work recently on the ground state of the $SU(2)$ antiferromagnet on the triangular lattice. For spin-1/2, there is good evidence [68, 69] that the ground state is quantum disordered. There are preliminary indications [80] that spin-Peierls order is absent in this state (which was predicted in Ref. [8] and discussed in Section 6.B.2), although larger system sizes are required before any firm conclusion can be reached. Another interesting issue of the kagomé is the nature of the large-spin magnetically ordered ground state selected by quantum fluctuations. A number of investigators [70, 71, 72, 73] have found the $\sqrt{3} \times \sqrt{3}$ discussed in Section 6.A.2.

7. CONCLUSIONS

It should be clear from all the discussion in this paper that there has been a great deal of progress in our understanding of non-random two dimensional antiferromagnets. The magnetically ordered states had been understood many years ago by semiclassical analyses. This course therefore focussed on recent work on the nature of the quantum phase transition to the quantum disordered phase and the properties of the quantum disordered phase itself. A partial classification of the different types of possible quantum disordered states has emerged, and was summarized in Section 6.D - the reader is urged to review this section, even if he/she did not have the patience to read the rest of Section 6. Also interesting was the fundamental connection between the properties of the quantum disordered states and the nature of the spin ordering in the magnetically ordered states.

Comparison of these results with experiments is complicated by the ubiquitous presence of randomness. Unlike classical systems, even weak randomness has a strong effect on the properties of quantum phase transitions and the low-energy properties of the quantum-disordered phase. In the renormalization group language, randomness is almost always a relevant perturbation at fixed points controlling the properties of quantum phase transitions and quantum-disordered phase. Our comparison with experiments has therefore been limited to a simple scaling analysis of phase transitions in random quantum antiferromagnets - this was summarized in Section 5. More detailed study of random quantum antiferromagnets is therefore clearly a high priority for future work. Recently, there has been some progress in solving random quantum magnets with infinite-range exchange interactions [24, 25]; a variety of unusual results were obtained, including the presence of gapless excitations in the quantum disordered phase. There have also been exact solutions of random quantum spin chains which are very instructive [81]. One hopes that these works are just the first stages of much further work on random quantum spin systems: the outlook for more interesting results is promising and the number of available experimental systems continues to grow.

Acknowledgements

I thank N. Read and Jinwu Ye for several fruitful collaborations which led to the work reviewed here. This research was supported by NSF Grant No. DMR-8857228 and by a fellowship from the A.P. Sloan Foundation.

References

- [1] H.A. Bethe, Z. Physik, **71** 205 (1991).
- [2] P.W. Anderson, Phys. Rev. B **86**, 694 (1952).
- [3] T. Nagamiya, R. Kubo, and K. Yosida, Phil. Mag., Suppl., **14**, 1 (1955).
- [4] P.W. Anderson, Science **235**, 1196 (1987).
- [5] J.G. Bednorz and K.A. Muller, Z. Phys. **B64**, 188 (1986); M.K. Wu *et. al.*, Phys. Rev. Lett. **58**, 908 (1987).
- [6] N. Read and S. Sachdev, Phys. Rev. Lett. **66**, 1773 (1991).
- [7] S. Sachdev and N. Read, Int. J. Mod. Phys. **B5**, 219 (1991).
- [8] S. Sachdev, Phys. Rev. B , **45**, 12377 (1992).
- [9] S.M. Hayden, G. Aeppli, H. Mook, D. Rytz, M.F. Hundley, and Z. Fisk, Phys. Rev. Lett. , **66**, 821 (1991).
- [10] S.-W. Cheong, G. Aeppli, T.E. Mason, H. Mook, S.M. Hayden, P.C. Canfield, Z. Fisk, K.N. Clausen, and J.L. Martinez, Phys. Rev. Lett. , **67**, 1791 (1991).
- [11] B. Keimer, R.J. Birgeneau, A. Cassanho, Y. Endoh, R.W. Erwin, M.A. Kastner, and G. Shirane, Phys. Rev. Lett. , **67**, 1930 (1991).
- [12] S.M. Hayden, G. Aeppli, R. Osborn, A.D. Taylor, T.G. Perring, S.-W. Cheong, and Z. Fisk, Phys. Rev. Lett. , **67**, 3622 (1991).
- [13] T.E. Mason, G. Aeppli, and H.A. Mook, Phys. Rev. Lett. , **68**, 1414 (1992).
- [14] T.R. Thurston, R.J. Birgeneau, Y. Endoh, P.M. Gehring, M.A. Kastner, H. Kojima, M. Matsuda, G. Shirane, I. Tanaka, and K. Yamada, MIT preprint.

- [15] B. Keimer, N. Belk, R.J. Birgeneau, A. Cassanho, C.Y. Chen, M. Greven, M.A. Kastner, A. Aharony, Y. Endoh, R.W. Erwin, and G. Shirane, MIT preprint.
- [16] M. Matsuda, Y. Endoh, K. Yamada, H. Kojima, I. Tanaka, R.J. Birgeneau, M.A. Kastner, and G. Shirane, MIT preprint.
- [17] A.P. Ramirez, G.P. Espinosa, and A.S. Cooper, Phys. Rev. Lett. , **64**, 2070 (1990).
- [18] C. Broholm, G. Aeppli, G.P. Espinosa, and A.S. Cooper, Phys. Rev. Lett. , **65**, 3173 (1990).
- [19] G. Aeppli, C. Broholm, and A. Ramirez in Proceedings of the Kagomé Workshop, NEC Research Institute, Princeton NJ.
- [20] D.S. Greywall, Phys. Rev. B **41**, 1842 (1990).
- [21] V. Elser, Phys. Rev. Lett. , **62**, 2405 (1990).
- [22] S. Sachdev and Jinwu Ye, Phys. Rev. Lett. **69**, 2411 (1992).
- [23] S. Chakravarty, B.I. Halperin, and D.R. Nelson, Phys. Rev. Lett. **60**, 1057 (1988); Phys. Rev. B **39**, 2344 (1989).
- [24] S. Sachdev and J. Ye, “Gapless spin-fluid ground state in a random quantum Heisenberg magnet”, paper 9212030 on cond-mat@babbage.sissa.it.
- [25] J. Ye, S. Sachdev, and N. Read, “A solvable spin-glass of quantum rotors”, paper 9212027 on cond-mat@babbage.sissa.it.
- [26] N. Read and S. Sachdev, Nucl. Phys. B**316**, 609 (1989).
- [27] *Coherent States* by J.R. Klauder and B. Skagerstam, World Scientific, Singapore (1985); see also *Generalized Coherent States and Their Applications*, by A. Perelomov, Springer-Verlag, New York (1986).
- [28] R. P. Feynman, Phys. Rev. **84**, 108 (1951).
- [29] F.D.M. Haldane, Phys. Lett. **93A**, 464 (1983); Phys. Rev. Lett. **50**, 1153 (1983); and J. Appl. Phys. **57**, 3359 (1985).
- [30] I. Affleck, Nucl. Phys. **B257**, 397 (1985); Nucl. Phys. **B265**, 409 (1985).
- [31] I. Affleck and F.D.M. Haldane, Phys. Rev **B36**, 5291 (1987).

- [32] X.G. Wen and A. Zee, Phys. Rev. Lett., **61**, 1025 (1988); E. Fradkin and M. Stone, Phys. Rev. **B38**, 7215 (1988); T. Dombre and N. Read, Phys. Rev. **B38**, 7181 (1988); R. Shankar and S. Sachdev, unpublished.
- [33] F.D.M. Haldane, Phys. Rev. Lett. **61**, 1029 (1988).
- [34] N. Read and S. Sachdev, Phys. Rev. Lett. **62**, 1694 (1989).
- [35] N. Read and S. Sachdev Phys. Rev. B **42**, 4568 (1990).
- [36] A.M. Polyakov, *Gauge Fields and Strings*, Harwood, New York (1987).
- [37] S. Sachdev and Jinwu Ye, unpublished.
- [38] S-k. Ma, *Modern Theory of Critical Phenomena*, Benjamin/Cummings, Reading (1976).
- [39] R. Abe, Prog. Thoer. Phys. **49**, 1877 (1973).
- [40] B. Keimer, private communication.
- [41] R.J. Gooding and A. Mailhot, Phys. Rev. B **44**, 11852 (1991); A. Aharony *et. al.*, Phys. Rev. Lett. **60**, 1330 (1988).
- [42] K. Binder and A.P. Young, Rev. Mod. Phys. **58**, 801 (1986).
- [43] G.A. Baker *et.al.* Phys. Rev. B **17**, 1365 (1978).
- [44] J.T. Chayes *et.al.* Phys. Rev. Lett. **57**, 2999 (1986).
- [45] D.S. Fisher, private communication.
- [46] G. Murthy and S. Sachdev, Nucl. Phys. **B344**, 557 (1990).
- [47] S.N. Dorogovstev, Phys. Lett. **76A**, 169 (1980); D. Boyanovsky and J.L. Cardy, Phys. Rev. B **26**, 154 (1982); I.D. Lawrie and V.V. Prudnikov, J. Phys. C, **17**, 1655 (1984).
- [48] C.C. Wan, A.B. Harris, and J. Adler, J. Appl. Phys. **69**, 5191 (1991).
- [49] R.N. Bhatt and P.A. Lee, Phys. Rev. Lett. **48**, 344 (1982).
- [50] I. Affleck, T. Kennedy, E.H. Lieb, and H. Tasaki, Phys. Rev. Lett. **59**, 799 (1987); D.Arovas, A. Auerbach and F.D.M. Haldane, Phys. Rev. Lett. **60**, 531 (1988).
- [51] D.P. Arovav and A. Auerbach, Phys. Rev. **B38**, 316 (1988); Phys. Rev. Lett. **61**, 617 (1988).

- [52] T. Einarsson and H. Johannesson, Phys. Rev. **B43**, 5867 (1991); T. Einarsson, P. Frojdh, and H. Johannesson, Phys. Rev. **45**, 13121 (1992).
- [53] P. Chandra, P. Coleman, and A.I. Larkin, Phys. Rev. Lett. **64**, 88 (1990); P. Chandra and P. Coleman, Int. J. Mod. Phys. **B3**, 1729 (1989).
- [54] B.I. Halperin and W.M. Saslow, Phys. Rev. B **16**, 2154 (1977).
- [55] T. Dombre and N. Read, Phys. Rev. B **39**, 6797 (1989).
- [56] P. Azaria, B. Delamotte, and T. Jolicoeur, Phys. Rev. Lett. **64**, 3175 (1990).
- [57] I. Affleck and J. Brad Marston, Phys. Rev. **B37**, 3774 (1988).
- [58] D. Rokhsar and S. Kivelson, Phys. Rev. Lett. **61**, 2376 (1988).
- [59] S. Sachdev, Phys. Rev. B **40**, 5204 (1989).
- [60] E. Fradkin and S. Kivelson, Mod. Phys. Lett. **B4**, 225 (1990).
- [61] S. Sachdev and R. Jalabert, Mod. Phys. Lett. **B4**, 1043 (1990).
- [62] C. Henley, Phys. Rev. Lett. **62**, 2056 (1989).
- [63] A. Chubukov, Phys. Rev. B **44**, 392 (1991).
- [64] F. Mila, D. Poilbanc, and C. Bruder, Phys. Rev. B **43**, 7891 (1991).
- [65] Similar incommensurate states with valence bonds connecting sites on the same sublattice are also found in a study of doped systems; B.I. Shraiman and E.D. Siggia, Phys. Rev. Lett. **62**, 1564 (1989); C. Jayaprakash, H.R. Krishnamurthy and S. Sarkar, Phys. Rev. B **40**, 2610 (1989); C.L.Kane *et al*, *ibid* **41**,2653 (1990); K. Feinsberg, P. Hedegard and M. Brix Pederson, *ibid* **40**, 850 (1989).
- [66] J. Stephenson, Can. J. Phys. **48**, 2118, 1724 (1970).
- [67] D. Yoshioka and J. Miyazaki, J. Phys. Soc. Jpn, **60**, 614 (1991); A. Kol and N. Read, unpublished
- [68] C. Zeng and V. Elser, Phys. Rev. B **42**, 8436 (1990).
- [69] R.R.P. Singh and D.A. Huse, Phys. Rev. Lett. , **68**, 1766 (1992).
- [70] A. Chubukov, Phys. Rev. Lett. , **69**, 834 (1992).

- [71] D.A. Huse and A.D. Rutenberg, Phys. Rev. B **45**, 7536 (1992).
- [72] A.B. Harris, C. Kallin, and A.J. Berlinsky, Phys. Rev. B **45**, 2889 (1992).
- [73] J.T. Chalker, P.C.W. Holdsworth, and E.F. Shender, Phys. Rev. Lett. , **68**, 855 (1992).
- [74] A.M. Polyakov, Nucl. Phys. **B120**, 429 (1977);
- [75] E. Fradkin and S.H. Shenker, Phys. Rev. **D19**, 3682 (1979).
- [76] W. Zheng and S. Sachdev, Phys. Rev. B **40**, 2704 (1989).
- [77] R.B. Laughlin, Science **242**, 525 (1988).
- [78] E. Dagotto and A. Moreo, Phys. Rev. Lett. **63** 2148 (1989); R.R.P. Singh and R. Narayan, Phys. Rev. Lett. **65**, 1072 (1990); A. Moreo, E. Dagotto, T. Joliceour, and J. Riera, Phys. Rev. B **42**, 6283 (1990); T. Ziman and H. Schulz, preprint
- [79] M.P. Gelfand, R.R.P. Singh, and D.A. Huse, Phys. Rev. B **40**, 10801 (1989); M.P. Gelfand, Phys. Rev. B **42**, 8206 (1990).
- [80] J.T. Chalker and J.F.G. Eastmond, Oxford preprint, OUTF-92-23S.
- [81] C.A. Doty and D.S. Fisher, Phys. Rev. **B45**, 2167 (1992); D.S. Fisher, Phys. Rev. Lett. **69**, 534 (1992); unpublished.